"Characterizing the space-time structure of rainfall in the Sahel with a view to estimating IDAF curves"

by Panthou et al (hess-2014-292)

We would first like to thank the anonymous reviewers for their comments. We have revised our manuscript in order to take into account to the largest extent, these comments. A point by point response is also provided below. We have also added a revised manuscript and a revised manuscript with tracks at the end of this response.

Anonymous Referee #1

The Authors investigate a not-easy issue represented by the space-time variability of rainfall, through the calculation of the Intensity-Duration-Area-Frequency (IDAF) curves. The area of interest is the Sahel region. The difficulty of this issue is also testified by the small number of contributions available in literature. Thus, this contribution is welcome.
The Authors use a simple scaling approach of annual maxima of rainfall in area and duration, and a GEV distribution for the description of annual maxima. The Authors apply the methodology to Sahel region verifying the hypotheses made. The manuscript sounds well from the technical point of view, however I found some issues to be fixed before its acceptance. Thus, I suggest a minor revision of the manuscript according to the comments reported in the next.

Detailed comments

1. Line 25 at page 8412, the reference De Michele et al (2002) is pertinent to this manuscript, similarly line 20 at page 8413. De Michele, C., Kottegoda, N.T., Rosso, R. 2002. IDAF(intensity-duration-area frequency) curves of extreme storm rainfall: a scaling approach. Water science and technology, 83-90.
Response : Done, we have added this reference in pages 8412 and 8413 (pages 3 and 5 of the revised manuscript).

2. In eq.(3), please change "z" with "i"
Response : We agree. We have replaced "z" by "i"

3. Lines 2-3 at page 8416, the sentence "the Areal Reduction Factor is the ratio between point rainfall and areal rainfall, either for a given observed rain event or in a statistical sense" is wrong. The Areal Reduction Factor is the ratio between areal rainfall and point rainfall for a given observed rain event. What do you mean for "in a statistical sense"? Similar consideration is applied to the sentence "this ARF thus denotes the ratio between the point distribution and the areal distribution of the annual rainfall maxima."
Response: In fact, when spanning the literature, it can be seen that the ARF terminology refers either to the ratio between areal rainfall and point rainfall for a given observed rain event or to the ratio between the point distribution and the areal distribution. It is exactly in that sense that de Michele et al. (2001) derive their ARF (see their data selection at the beginning of their section 5.). The review produced by Svensson and Jones (2010) explains comprehensively the

different ways of computing an ARF found in the literature. Bell (1976; see the first lines of section 3.3) defines the ARF as the ratio between the point rainfall for a given return period and the areal rainfall corresponding to the same return period. By specifying in our paper that we deal with the ARF issue "in a statistical sense", we intent to make clear to the reader that we look at ratios of distributions or ratios of statistics rather than at ratios of observed rainfall for a given event.

Bell, F. (1976), The areal reduction factor in rainfall frequency estimation, Tech. rep., Institute of hydrology, Natural Environment Research Council, UK.
De Michele, C., N. T. Kottegoda, and R. Rosso (2001), The derivation of areal reduction factor of storm rainfall from its scaling properties, Water Resour. Res., 37(12), 3247–3252.
Svensson, C., and D. A. Jones (2010), Review of methods for deriving areal reduction factors, J. Flood Risk Manag., 3(3), 232–245.

4. In Eq.(15), please define μ_{ref}, In Eq.(16), please define σ_{ref} In Eq.(17), please define ξ_{ref}
Response : We have defined the three symbols after Equation 17 in the following way : "*where μ_{ref}, σ_{ref} , and ξ_{ref} correspond to the GEV parameters computed for the arbitrary reference duration D_{ref}*". Note that D_{ref} is introduced for the first time in line 21 page 8414) ; in our case study, this reference duration happens to be one hour.

5. According to Eq.(13), in Eq.s(15-17), I think that the subscript "ref" must be substituted with "1". Some clarifications are necessary here.
Response : Equations (15-17) are general equations; they are not specific to the case study we are treating here. This is why it is indeed correct to use μ_{ref}, σ_{ref} , and ξ_{ref} rather than μ_1, σ_1 , and ξ_1 in these equations.

6. Page 8418, line 6, I suggest to delete "initial"
Response : We deleted "initial".

7. Page 8418, lines 22-23, the definition of r(x,y,t) can be ambiguous. 1) The Authors write "we denote by r(x,y,t) the actual 5-min rainfall accumulation recorded at a given time t and at a given rain gauge of coordinates (x,y)." It is not clear if the instant "t" is the starting point or the ending instant of the 5-min interval. 2) r(x,y,t) should be the instantaneous rainfall recorded at a given time t. Presently r(x,y,t)= rD=5(x,y,t), but this is not clear in the manuscript.
Response : We agree. We have thus modified lines 22-23 page 8418 (page 10 of the revised manuscript) as follows:

"*The starting elements of the space-time aggregation process, are the discretized fields of rain accumulated over a time increment Δt = 5 min and averaged over a square-pixel of side length Δxy = 1 km. In the following, these rainfields are denoted as r*(x*, y*, t*), where t* is the ending time of the 5-min time-step, and {x*, y*} is the center of the 1 km^2 pixel.*"

Accordingly, we have slightly changed the two following sections (3.2.1 and 3.2.2) and eq. 18-20 (pages 10-11 of the revised manuscript).

8. Page 8423, line 26, for large areas (900, 1600 and 2500 km2) you have also the problem that increasing the area, you could include more than one single center of storm, and consequently also the definition of ARF is difficult. Similar problems, for large areas, are found also in De Michele et al. 2001, 2002.

Response : As mentioned earlier, our definition of the ARF refers to the ratio between the point rainfall for a given return period and the areal rainfall (centered on the rain gauge where the point distribution is extracted) for the very same return period. This is why it was important to specify "in a statistical sense" in our definition of the ARF: it is a statistical integration of various situations in terms of rainfall spatial distribution: single storm with continuous rainfall, single storm with intermittent rainfall in space, storms with several peaks in space and/or times, several storms at the same moment in the area of integration, … This is the most robust and consistent way to define the ARF because it does not refer to any specific configuration of the rainfall events, but rather integrates all the encountered situations.

9. Page 8423, please provide some comments about the value of the parameters obtained, and in particular the dynamic scaling exponent.

Response: We have produced a table containing the obtained parameters and added the following comment page 8423 (page 15 of the revised manuscript - just before section 5) : "*Table 1 presents the parameters obtained for the global IDAF model. The obtained GEV parameters are* μ_{rej}*= 40.6 mm/1h,* σ_{rej} *= 10.8 mm/1h, and* $\xi = 0.1$*. When upscaled to the daily duration* $\mu(24h) = 2.29$ *mm/h (55.0 mm/d) and* $\sigma(24h) = 0{,}61$ *mm/h (14.6 mm/24h). It is worth noting that these latter values are coherent with those obtained for a much larger area in this region by Panthou et al. (2012, 2013), working on the data of 126 daily rain gauges covering the period 1950-2010. Note also that the temporal scale exponent (η) is large (0.9), which means that the intensity strongly decreases as the duration increases. This is not surprising given the strong convective nature of rainfall in this region. Similar values of the temporal scaling exponents are obtained in regions where strong convective systems occur [Mohymont et al., 2004; Van-de -Vyver and Demarée, 2010; Ceresetti et al., 2011] while lower values are obtained in regions where extreme rainfall is generated by different kinds of meteorological systems (for example in many mid-latitudes regions, see e.g. Menabde et al., 1999; Borga et al., 2005; Nhat et al., 2007). The dynamic scaling exponent is roughly equal to 1 which means that increasing the surface by a given factor leads to a similar ARF change than increasing the duration by the same factor (keeping in mind that this rule applies only to the range of time-space resolutions explored here)*".

Borga, M., C. Vezzani, and G. D. Fontana (2005), Regional rainfall depth-duration-frequency equations for an Alpine region, Nat. Hazards, 36(1), 221–235.

Ceresetti, D., S. Anquetin, G. Molinié, E. Leblois, and J. D. Creutin (2011), Multiscale Evaluation of Extreme Rainfall Event Predictions Using Severity Diagrams, Weather Forecast., 27(1), 174–188.

Menabde, M., A. Seed, and G. Pegram (1999), A simple scaling model for extreme rainfall, Water Resour. Res., 35(1), 335–339.

Mohymont, B., G. R. Demarée, and D. N. Faka (2004), Establishment of IDF-curves for precipitation in the tropical area of Central Africa-comparison of techniques and results, Nat. Hazards Earth Syst. Sci., 4(3), 375–387.

Nhat, L. M., Y. Tachikawa, T. Sayama, and K. Takara (2007), A simple scaling charateristics of rainfall in time and space to derive intensity duration frequency relationships, Annu. J. Hydraul. Eng., 51, 73–78.

Panthou, G., T. Vischel, T. Lebel, J. Blanchet, G. Quantin, and A. Ali (2012), Extreme rainfall in West Africa: A regional modeling, Water Resour. Res., 48(8), 1–19.

Panthou, G., T. Vischel, T. Lebel, G. Quantin, A.-C. Pugin, J. Blanchet, and A. Ali (2013), From pointwise testing to a regional vision: An integrated statistical approach to detect nonstationarity in extreme daily rainfall. Application to the Sahelian region, J. Geophys. Res. Atmospheres, 118, 8222–8237.

Van-de-Vyver, H., and G. R. Demarée (2010), Construction of Intensity-Duration-Frequency (IDF) curves for precipitation at Lubumbashi, Congo, under the hypothesis of inadequate data, Hydrol. Sci. J.-J. Sci. Hydrol., 55(4), 555–564.

10. Page 8424, line 18. Question: how you have calculated the critical values of the KS and AD tests? The issue is not trivial because the authors have estimated the parameters from the data. Please provide details on this issue.

Response : This is a good point. We have therefore re-computed the KS and AD tests by using a classical leave-one-out cross validation procedure: all the stations are used to calibrate the model except one which is used to validate the model prediction. The process is carried out for all stations. Thus, the GOF tests are now computed on data that have not been used to fit the model.

The results are very similar to those obtained previously and we have thus substituted this new figure to the previous figure 9.

Line 15 of Page 8424 (lines 13-15 page 16 of the revised manuscript) was accordingly changed to: "and by using Goodness Of Fit (GOF) statistical tests computed in a cross validation mode (all the stations are used to calibrate the model except one which is used to validate the model prediction)"

11. Page 8427 line 8. Please provide some references for "copulas".

Response: We have added two references. It now reads : "*Therefore developing an IDAF model able to account for a possible evolution of the ARF with the return period level is a path that has to be explored, copulas being a candidate for such a development (e.g. Singh and Zhang, 2007; Ariff et al., 2012)* ."

Singh, V. and Zhang, L. (2007). "IDF Curves Using the Frank Archimedean Copula." J. Hydrol. Eng., 12(6), 651–662.

Ariff, N., Jemain, A., Ibrahim, K., and Wan Zin, W. (2012). "IDF relationships using bivariate copula for storm events in Peninsular Malaysia." Journal of Hydrology, 470-471, 158-171.

12. Page 8436, Figure 4, change "E[i(d)q]" with "E[Iq(D)]". Same comment to page 8437, Figure 5.

Response : Done. We have also corrected this point in the text (e.g. page 8423 line 12).

13. Page 8439, Figure 7, indicate the random variable with the capital letter "I".

Response : Done

Anonymous Referee #2

This paper presents a global model to define intensity duration area frequency curves, based on simple scaling in space and time in combination with dynamic scaling to relate space and time. The model is applied to a network of rain gauges in the Sahel region with 22 year time series of rainfall data. Hypotheses underlying the model are verified and discussed in a thorough way. Some improvements could still be made to improve consistency and clarity of the paper, that I suggest could be made in a minor review of the paper.

1- Variable symbols are not used consistently in equations throughout the manuscript and explanations of several variables are missing, especially: ζ (eq 2); σ is both scale and shape parameter? (in eq 2); η (in eq 4); q, k(q) (eq 6); λ (in l1 p 8415 is explained for eq 4, but eq 4 does not have a λ?); η seems to be used in a different sense in eq 13 to 17 compared to eq 4.

Response: These remarks are puzzling, except regarding equation 6, where the definition of q and k(q) is missing (corrected); we wonder whether the printing of the manuscript did not yield errors in the restitution of the equations (as reviewers we have had similar experiences with HESS manuscripts). If the equations are correctly printed, it will be seen that Equation 2 is the basic standard equation of the GEV model, with ζ being clearly the shape parameter and σ the scale parameter. These two parameters are used as such consistently all through the manuscript. Equation 4 does have a λ. Finally, η is the classical scale exponent used in every simple scaling model; it has the same meaning in equation 4 and in equations 13 to 17.

2- On page 8411 various references to papers working on IDF and IDAF curves have been mentioned; it would be good to include reference to recent studies using radar-rainfall data for space-time analysis of rainfall (e.g. mention Overeem et al. (2009) here 1)

Response: Thanks for the suggestion. We added this reference page 8411 (page 3, line 13 of the revised manuscript): "*IDF practical studies are also numerous but focused on regions where long series of sub-daily rainfall are available (e.g. Borga et al., 2005; Gerold and Watkins, 2005; Nhat et al., 2007; Bara et al., 2009; Ben-Zvi, 2009; Overeem et al. 2009; Awadallah, 2011; Ariff et al., 2012).* "

Overeem, Aart, T. A. Buishand, and Iwan Holleman. "Extreme rainfall analysis and estimation of depth-duration-frequency curves using weather radar." Water resources research 45.10 (2009).

3- On page 8418, the initial rainfall dataset is discussed. It is stated that all years where more than 25% of data were missing were excluded from analysis. Please clarify if this 25% includes 0 rainfall data or refers to >0 mm rainfall data points (if so, what was the applied threshold)? If 25% data includes 0 rainfall, a lot of relevant (significant) rainfall data points could still be missed. Could the authors elaborate a bit more on this, especially given the rather exceptional rainfall regime of the region?

Response: The 25% missing data include 0 rainfall, which of course leaves room to the possibility of missing some extreme rainfall in our sample. This is unavoidable and one can only assume that on a sample of 690 station-years, the distribution of sampling of missing data is not significantly different from the overall sampling distribution. Thus the key point is whether a 25% threshold is appropriate. With respect to this point one has to bear in mind that many recording problems occur at the beginning of the rainy season, due to the dust that is transported by strong winds blowing on a dry and nude surface. This relatively high threshold takes into account this specificity of the rainfall regime of the region.

4- On page 8419:
4a. Spatial aggregation of the rainfall fields: please clarify how rainfall data were spatially aggregated - were data simply averaged, were any spatial weights applied?
4b Later, in lines 15-16 it is stated that " only rain gauges having at least 1 other rain gauge present in at least seven of the eight sectors are retained". This could hardly be true for smaller spatial aggregations (rain gauge density is too low at these scales to meet this requirement) – please explain
Response:

4a. Spatial weighting is applied when constructing the 5-min. rainfields, following the dynamical kriging method of Vischel et al. (2011). In order to clarify this point the sentence "*this study makes use of the dynamical interpolation method*" was replaced by "*this study makes use of the dynamical kriging interpolation method*". Once these *elementary* 5-min. rainfields are produced, no further spatial weighting is applied (nor is it needed) when computing the areal rainfall over the squares of various sizes.

4b. We must acknowledge that our explanation was somewhat confusing. We first refer to "*stations surrounded by a sufficient number of rain gauges*" and then we explain that the selection is carried out on a direction criterion. We hope to have clarified this point by re-writing the explanation as follows:

"*To limit border effects, the spatial aggregation is performed only in areas where the spatial distribution of stations is more or less isotropic. Each of the 30 measurement stations is considered individually; a circle centered on the station is plotted and divided in eight cardinal sectors (each sector has an angle of 45°). Only rain gauges having at least one other rain gauge present in at least seven of the eight sectors are retained for spatial aggregation; the distance of the other gauges from the center station is not taken into account for the selection, only matters the presence or absence of a rain gauge in the sector. Only 13 gauges (out of 30) satisfy this criterion (Fig. 1). They are referred to in the following as central rain-gauges (CR) because their localization is used as a central point, from which the 12 areas of aggregation are delimited. In total there are thus 156 areal series (12 areas of aggregation centered on 13 different locations)"*

Figure 3a was also changed in order to better explain the procedure.

Vischel, T., G. Quantin, T. Lebel, J. Viarre, M. Gosset, F. Cazenave, and G. Panthou (2011), Generation of High-Resolution Rain Fields in West Africa: Evaluation of Dynamic Interpolation Methods, J. Hydrometeorol., 12(6), 1465–1482.

P5- Page 8420: lowest temporal resolution used is 1 hour, while original data have 5 min resolution. Why were smaller temporal resolutions (15 min, 30 min) not considered?
Response: This choice was made in order to lie on the safe side on two points:

i) The lower is the time step, the greater is the potential error on the intensities; below 30 minutes these errors might become large enough to undermine the consistency of statistical studies such as the one carried out here

ii) We also expect a different scaling behavior for shorter durations than 1 hour

6- On page 8422, it is stated that "methods takes advantage of limiting sampling effects by

increasing sample size". This is not entirely true: the same number of samples are aggregated over a range time windows to obtain datasets of different temporal resolutions;
this does not increase sample size.
Response: This is correct, the same number of series were temporally and spatially aggregated. We have modified this sentence. It now reads: "In comparison with fitting the GEV parameters separately to each sample constituted for each duration, this method aims at limiting sampling effects by fitting the GEV parameters on a single sample gathering all rainfall durations."

7- On page 8422, l 20-21: it is stated that "the obtained IDF and IDAF curves do not display either any coherent spatial pattern or any trend over the domain". It would be helpful to illustrate this in a figure and to verify this statement in a more formal way: checking statistical differences in parameters of the IDF/IDAF distributions across the spatial domain.
Response: We have added a map for each parameter of the IDF/IDAF model obtained. We have thus modified the sentence: "*the obtained IDF and IDAF curves do not display either any coherent spatial pattern or any trend over the domain, as may be seen in Figure 5*."

8- On page 8423: please report and discuss values of the parameters obtained, especially the dynamical scaling
Response: Reviewer #1 has also made this point. See our response to comment #9 of reviewer #1.

9- Discussion: The authors state that rain gauge networks continue to have an important value for space-time rainfall information in generating long time series of rainfall. Such networks however have the disadvantage of uncertainty introduced by spatial interpolation that for instance radars do not have. Can the authors please discuss the influence of uncertainty introduced by interpolation of rain gauge data on IDAF curves and how this compares to resolutions that could be obtained from radar information. And also to what extent a region like the Sahel would benefit from higher resolution data (either obtained from radar or denser rain gauge networks).
Response: It is a matter of fact that, at present, only high quality recording rain gauge series can provide a long term perspective on extreme rainfall regimes and their possible evolution in many regions of the world and especially in West Africa. Despite the fact that radars were/are installed on some airports, their operation and maintenance were never sufficient for providing long term continuous series that could have been used in a study like the one presented here. And it will be some time before a consistent set of modern meteorological radars is available in this region. Therefore, our main argument is that, at present, maintaining high quality recording rain gauge networks should be a priority of the scientific community working in the region. When other sensors appear able to provide consistent long series of areal rainfall measurements, then it will be time to consider how best such measurements should be complemented by gauge measurements for validation purpose and for keeping some continuity with measurements of the past.

Assume now that we are living in a theoretical world where there are long series of good quality radar measurements available in West Africa. Our opinion is that long series of good quality gauge measurements would still be desirable. The reviewer is right to point to the uncertainty introduced by the spatial interpolation of point measurements. And even if we can compute theoretical standard deviations of errors based on the best linear unbiased estimation

theory, it is certainly very difficult to introduce these errors in the regional GEV model and to assess their impact on the quality of the scaling relationships that we have computed. On the other hand, radar rainfall estimates are not devoid of their own errors linked to both measurement and sampling (even developed countries that have been operating radar for decades, are maintaining gauge networks for climatological and hydrological purposes). Thus confronting the scaling models that would be computed from gauge networks, on the one hand, and from radar series, on the other hand, is a very appealing perspective that is probably possible now in countries that have been operating good quality radar for years (do not forget, by the way, that radars were continuously improved over years and that it is not easy to work on homogeneous series of radar data).

Comments on figures:

10- Figures are small and sometimes difficult to read. Figures 4 to 8 are quite dense and would benefit from more explanation in the figure captions. Overall, more information in figure captions is needed to properly understand what is shown; preferably, figures should be clear, independent of the text.
Response: We have modified the captions of Figures 4 to 8

The new captions are:

Figure 4. Example of IDAF model inference at the Niamey Aeroport Rain gauge: a) Checking of the temporal simple scaling conditions (left: linear relationship between the logarithm of the statistical moments of order q and the durations D, right: linear relationship between k(q) and q) and estimation of the temporal simple scaling exponent; b) left: empirical cumulative distribution of annual maxima, right: global fitting of the GEV parameters; c) Comparison between empirical and modelled ARF .

Old Figure 5 (new figure 6). Checking of the temporal simple scaling conditions for the regional samples defined by the 30 available rain gauges for point resolution (top), and the 13 CR rain gauges (see Section 3.2.1) for the resolutions 100 km^2 (middle) and 2500 km^2 (bottom).

Old Figure 6 (new figure 7). Comparison between empirical ARF (obtained with the regional samples: 30 rain gauges for point resolution and 13 CR rain gauges for other spatial resolutions) and modelled ARF IDAF model.

Old Figure 7 (new figure 8). Comparison between empirical mean areal rainfall intensity (obtained with the regional samples: 30 rain gauges for point resolution and 13 CR rain gauges for other spatial resolutions) and global IDAF model for different spatio-temporal aggregations.

Old Figure 8 (new figure 9). Empirical return level plot obtained at two rain gauges in comparison with the global IDAF model for different durations (1h, 6h and 24h from top to bottom) and different spatial aggregations (from point to 2500 km^2).

11- In figure 2 and 4, the first moment seem to be decreasing with increasing duration, which could be a boundary effect. Please explain.

Response: Since the rainfall intensity (and not the rainfall depth) is considered in this study, it is absolutely normal that the moments decrease as the duration increases (Figure 2 left panel and Figure 4).

However, the reviewer is right that in the central graphic of Figure 2 – which is only an illustrative example – (k(q) values should have been negatives and decreased as q increases: this was corrected.

Manuscript prepared for Hydrol. Earth Syst. Sci. Discuss.
with version 2014/05/30 6.91 Copernicus papers of the LaTeX class copernicus.cls.
Date: 17 October 2014

Characterizing the space–time structure of rainfall in the Sahel with a view to estimating IDAF curves

G. Panthou, T. Vischel, T. Lebel, G. Quantin, and G. Molinié

LTHE – UMR5564, Univ. Grenoble, IRD, CNRS, Grenoble, France

Correspondence to: T. Vischel (theo.vischel@ujf-grenoble.fr)

Abstract

Intensity–duration–area–frequency (IDAF) curves are increasingly demanded for characterizing the severity of storms and for designing hydraulic structures. Their computation requires inferring areal rainfall distributions over the range of space–time scales that are the most relevant for hydrological studies at catchment scale. In this study, IDAF curves are computed for the first time in West Africa, based on the data provided by the AMMA-CATCH Niger network, composed of 30 recording rain gauges having operated since 1990 over a 16 000 km^2 area in South West Niger. The IDAF curves are obtained by separately considering the time (IDF) and space (Areal Reduction Factor – ARF) components of the extreme rainfall distribution. Annual maximum intensities are extracted for resolutions between 1 and 24 h in time and from point (rain-gauge) to 2500 km^2 in space. The IDF model used is based on the concept of scale invariance (simple scaling) which allows the normalization of the different temporal resolutions of maxima series to which a global GEV is fitted. This parsimonious framework allows using the concept of dynamic scaling to describe the ARF. The results show that coupling a simple scaling in space and time with a dynamical scaling relating space and time allows modeling satisfactorily the effect of space–time aggregation on the distribution of extreme rainfall.

1 Introduction

Torrential rain and floods have long been a major issue for hydrologists. For one, defining and computing their probability of occurrence is a scientific challenge *per se*, largely because it is a scale-dependent exercise. Secondly, and as important, is the fact that they cause heavy environmental, societal, and economical damages – including human losses – thus being a major concern for populations and decision makers.

The request of providing both an objective assessment of the probability of occurrence of high impact rainfall and a tool for civil engineering structure design has found an answer through the calculation of intensity–duration–frequency (IDF) curves. These curves, generally computed from rain gauge data, are intended at characterizing the evolution of extreme rainfall distribu-

tions at a point when the duration of rainfall accumulation changes. However rainfall at point location is not of greatest interest when it comes to the hydrological and socio-economic impacts of extreme events, since it is essentially the convolution of the rainfall intensities over a catchment that characterizes the severity of storms and creates the real threat.

This is why intensity–duration–area–frequency (IDAF) curves were conceived as a spatial extension of the IDF curves. Generally established by combining IDF curves and Areal Reduction Factors (ARF), they provide an estimation of extreme areal rainfall quantiles over a range of time and spatial scales.

Theoretical studies on IDF and ARF have been an active research topic over the past 20 years or so (Koutsoyiannis et al., 1998; Menabde et al., 1999; De Michele et al., 2001, 2011, among others). IDF practical studies are also numerous but focused on regions where long series of sub-daily rainfall are available (e.g. Borga et al., 2005; Gerold and Watkins, 2005; Nhat et al., 2007; Bara et al., 2009; Ben-Zvi, 2009; Overeem et al., 2009; Awadallah, 2011; Ariff et al., 2012). On the other hand, when ARF are computed from rain gauge networks (Bell, 1976; Asquith and Famiglietti, 2000; Allen and DeGaetano, 2005), it requires a fair density of rain gauges in order to obtain accurate estimates of areal rainfall. The computation of IDAF curves must therefore deal with two major data requirements: (i) a high density network of rain gauges having produced and (ii) an array of long subdaily rainfall series. In addition to these requirements, scientists face the challenge of producing coherent ARF and IDF models, if they wish their IDAF model to be statistically consistent. This explains why there are so few studies dealing with the implementation of an IDAF model over a given region (e.g. De Michele et al., 2002; Castro et al., 2004; De Michele et al., 2011; Ceresetti, 2011).

In fact, in some regions of the world there are virtually no IDF, ARF and IDAF models that have ever been conceived because of data limitations. This is especially the case in many tropical regions, such as West Africa, one reason being that a harsh environment and resource scarcity have make very challenging the operation of recording rain gauge networks. The few IDF studies available in the region (Oyebande, 1982; Mohymont et al., 2004; Oyegoke and Oyebande, 2008; Soro et al., 2010) are essentially empirical with no theoretical background allowing to upgrade their results in order to produce IDAF curves. ARF studies are still fewer,

the most noticeable being an attempt by Rodier and Ribstein (1988) and Ribstein and Rodier (1994) at computing ARF values for a return period of 10 years, with no explicit inference of the areal rainfall distributions. All in all, there has never been any IDAF model derived for West Africa or sub-regions of West Africa. Yet, flood management – for which IDAF curves are a very useful tool – is now a major concern for West African countries. As a matter of fact and despite that West Africa is known for having experienced a major lasting drought over 1970–2000, numerous severe floods and exceptional inundations have struck the region over the last two decades (Tarhule, 2005; Descroix et al., 2012; Samimi et al., 2012). Moreover, the flood damages in the region have been in constant increase since 1950 (Di-Baldassarre et al., 2010).

While operational networks of the West African National Weather Services do not allow the establishment of IDAF curves in a consistent way – because they do not provide any long term subdaily rainfall series – there are other sources of data that can be used for that purpose. Among them are the 5-min rainfall series of the long term AMMA-CATCH observing system covering a 16 000 km^2 area in South West Niger from 1990 onwards (Fig. 1). In this study we will make use of 30 series providing continuous 5-min rainfall records from 1990 to 2012.

This unique data set enables us to characterize the relationship between extreme rainfall distributions computed at various spatio-temporal scales and to propose IDAF curves for this characteristic Sahelian region.

2 IDAF curves in a GEV distribution and scale invariance framework

IDAF curves are providing an estimate of areal rain-rates – averaged over a given duration D and a given area A – for a given frequency of occurrence (currently expressed in term of return period T_r). In practice, IDAF curves are generally obtained by aggregating a temporal component and a spatial component represented respectively by the intensity–duration–frequency curves (IDF) computed at a point ($A = 0$) and by the Areal Reduction Factors (ARF) computed for a range of duration. In this framework, the most general formulation of an IDAF equation is as follows:

$$\mathrm{IDAF}(D, A, T_\mathrm{r}) = \mathrm{IDF}(D, T_\mathrm{r}) \times \mathrm{ARF}(D, A, T_\mathrm{r}). \quad (1)$$

Assessing IDAF curves requires: (i) inferring appropriate statistical distributions of rainfall to estimate the return periods and (ii) describing the statistical links between the distributions obtained at different space–time scales.

Several recent studies have confirmed that the Generalized Extreme Value (GEV) distribution (Coles, 2001) provides a suitable framework to describe the distribution of extreme rainfall at a point (e.g. Overeem et al., 2008; Panthou et al., 2012; Papalexiou and Koutsoyiannis, 2013). Also, many authors have shown that rainfall displays scale invariance properties (Schertzer and Lovejoy, 1987; Gupta and Waymire, 1990; Burlando and Rosso, 1996; Bendjoudi et al., 1997; Veneziano et al., 2006); both in space and time. The temporal scaling properties give access to a direct analytical formulation of IDF curves (Menabde et al., 1999; Borga et al., 2005; Ceresetti, 2011), while the spatial scaling properties allow to upscale IDF curves into IDAF curves (De Michele et al., 2002; Castro et al., 2004; De Michele et al., 2011), thus providing an integrated space–time characterization of extreme rainfall distributions. Under certain assumptions, namely the GEV distribution of point annual rainfall maxima and simple scaling in both time and space, an analytical formulations of the various components of Eq. (1) may be obtained, as will be detailed below.

2.1 GEV distribution

Let us define $I(D,A)$ a random variable representing the annual maxima of rainfall accumulated over a given duration D and area A, and $i(D,A)$ a sample of $I(D,A)$. In the general framework of the block maxima sampling scheme (Coles, 2001), working on annual maxima generally ensures that the block size is large enough for the maxima distribution to follow a GEV distribution (Coles, 2001), written as:

$$G(i;\mu,\sigma,\xi) = \exp\left\{-\left[1+\xi\left(\frac{i-\mu}{\sigma}\right)\right]^{-\frac{1}{\xi}}\right\} \quad \text{for } 1+\xi\left(\frac{i-\mu}{\sigma}\right) > 0 \tag{2}$$

where i is a generic notation for any value associated with a realization of $I(D,A)$, μ being the location parameter, $\sigma > 0$ the scale parameter and ξ the shape parameter of the GEV distribution. The shape parameter describes the behavior of the distribution tail: a positive (resp.

negative) shape corresponds to a heavy tailed (resp. bounded) distribution. When ξ is equal to 0, the GEV reduces to the Gumbel distribution (light tailed distribution):

$$G(i;\mu,\sigma) = \exp\left\{-\exp\left[-\left(\frac{i-\mu}{\sigma}\right)\right]\right\}. \quad (3)$$

2.2 Simple scaling in time and analytical formulation of IDF curves

The simple scaling framework has been extensively used for deriving IDF curves (Menabde et al., 1999; Yu et al., 2004; Borga et al., 2005; Nhat et al., 2007; Bara et al., 2009; Ceresetti, 2011). It provides a much more tractable analytical framework than the multi-scaling approach and is more robust in terms of parameter inference.

The annual maximum point rainfall random variable $\{I(D,0)\}$ follows a simple scaling relation for a given duration D – with respect to a reference duration D_{ref} – if:

$$I(D,0) \overset{d}{=} \lambda^{\eta} \times I(D_{\text{ref}},0) \quad (4)$$

where λ is a scale ratio ($\lambda = D/D_{\text{ref}}$), η is a scale exponent and $\overset{d}{=}$ denotes an equality in distribution. Note that, for every duration D for which Eq. (4) holds, the normalized random variable $\{I(D,0)/D^{\eta}\}$ has the same statistical distribution than the normalized reference distribution $\{I(D_{\text{ref}},0)/D_{\text{ref}}^{\eta}\}$; this property will be used in the optimization procedure, in Sect. 4.2. Equation (4) implies (Gupta and Waymire, 1990):

$$E[I(D,0)] = \lambda^{\eta} \times E[I(D_{\text{ref}},0)] \quad (5)$$

and, more generally, a scaling of all the moments, that can be written as:

$$E[I^q(D,0)] = \lambda^{k(q)} \times E\left[I^q(D_{\text{ref}},0)\right]. \quad (6)$$

Or:

$$\ln\{E[I^q(D,0)]\} = k(q)\ln(\lambda) + \ln\left\{E\left[I^q(D_{\text{ref}},0)\right]\right\}. \quad (7)$$

The notion of simple scaling is related to how $k(q)$ evolves with q. When this evolution is linear:

$$k(q) = \eta q \tag{8}$$

then simple scaling holds (as opposed to multi-scaling if this relation in non linear).

Checking whether the simple scaling hypothesis is admissible over a given range of durations is thus equivalent to verifying on the data set whether the two following conditions are fulfilled (Gupta and Waymire, 1990):

- Eq. (7): log–log linearity between the statistical moments of any given order q;
- Eq. (8): linearity between $k(q)$ and q, $\eta(= k(1))$ being the scaling factor at order 1.

Figure 2a illustrates these two conditions.

2.3 Spatial scaling, dynamical scaling and ARF model

In its most general sense, the Areal Reduction Factor is the ratio between point rainfall and areal rainfall, either for a given observed rain event or in a statistical sense. Here we are interested in deriving a statistical ARF that can be used for obtaining an analytical formulation of IDAF curves (which implies that the ARF does not depend on the return period considered); this ARF thus denotes the ratio between the point distribution and the areal distribution of the annual rainfall maxima:

$$I(D,A) \stackrel{d}{=} \mathrm{ARF}(D,A) \times I(D,0). \tag{9}$$

Note that Eq. (9) implies the following relationship:

$$\mathrm{ARF}(D,A) = \frac{E[I(D,A)]}{E[I(D,0)]}. \tag{10}$$

In this study, the ARF model proposed by De Michele et al. (2001) is used. This model is based on two assumptions (which will have to be verified, see Sect. 5):

1. the studied rainfall variable is characterized by a simple scaling relationship both in time and space;

2. time and spatial scales are linked by a so-called dynamic scaling property written as:

$$\left(\frac{D}{D_{\text{ref}}}\right) = \left(\frac{A}{A_{\text{ref}}}\right)^{z} \tag{11}$$

where z is the dynamical scaling exponent.

When these assumptions are verified, De Michele et al. (2001) show that the ARF can be written as:

$$\text{ARF}(D,A) = \left[1+\omega\left(\frac{A^a}{D^b}\right)\right]^{\eta/b} = \left[1+\omega\left(\frac{A^z}{D}\right)^b\right]^{\eta/b} \tag{12}$$

where:

- η is the scaling exponent characterising the temporal simple scaling;
- a and b are two positive constant scaling exponents linked by the relation $z = a/b$;
- ω is a factor of normalization.

This ARF formulation implies that iso-ARF are lines in the plane $\{\ln(A), \ln(D)\}$ as shown in Fig. 2b (De Michele et al., 2001).

2.4 GEV simple scaling IDAF model

By assuming that the maximum annual rainfall is GEV-distributed and that the scaling relations in time and space (Sects. 2.2 and 2.3) are verified, then the IDAF model is:

$$I(D,A) \stackrel{d}{=} I(D_{\text{ref}},0) \times \lambda^{\eta} \times \text{ARF}(D,A). \tag{13}$$

As shown in the Appendix A, the compatibility of the simple scaling and GEV frameworks is defined by the following equations:

$$I(D,A) \sim \text{GEV}\{\mu(D,A),\sigma(D,A),\xi(D,A)\} \tag{14}$$

$$\mu(D,A) = \mu_{\text{ref}} \times D^{\eta} \times \text{ARF}(D,A) \tag{15}$$

$$\sigma(D,A) = \sigma_{\text{ref}} \times D^{\eta} \times \text{ARF}(D,A) \tag{16}$$

$$\xi(D,A) = \xi_{\text{ref}} \tag{17}$$

where μ_{ref}, σ_{ref} , and ξ_{ref} correspond to the GEV parameters computed for the arbitrary reference duration D_{ref}.

3 Data and implementation

Rainfall observing systems usually do not provide direct measurements at all the space and time scales required for an IDAF study; it is thus needed to derive from the raw data set, an elaborated data set that will allow verifying the various assumptions founding the theoretical framework defined in Sect. 2.

Accordingly, this section describes both the rainfall samples initially available on our Sahelian region of South-West Niger and the process used to obtain the final data set from which the IDAF curves were computed. This process consists in two major steps:

1. Space–time aggregation of the 5-min point rain-rates in order to obtain the average rain-rates for various space (A) and time (D) resolutions;
2. Extraction of extreme rainfall samples for each of the above resolutions.

3.1 The rainfall data set: AMMA-CATCH Niger records

The AMMA-CATCH Niger observing system was set up at the end of the 1980s as part of the long term monitoring component of the Hapex-Sahel experiment (Lebel et al., 1992). Since

then, it has operated continuously a large array of meteorological and hydrological instruments, providing a unique set of high resolution hydrometeorological data, covering a 16 000 km^2 area in South West Niger. For the purpose of this research, a subset of 30 5-min rainfall series was selected (Fig. 1), covering the entire 1990–2012 period. At each station, all year with more than 25 % of missing data have been removed in order to limit any sampling effect due to missing data in a particular year. After this quality control, all stations remain with at least 20 years of valid data, constituting our raw data sample.

To estimate areal rainfall intensities, this study makes use of the dynamical kriging interpolation method proposed by Vischel et al. (2011). Rainfields are produced over the domain of study at a time resolution of 5 min and a spatial resolution of 1 km^2.

3.2 Space–time rainfall aggregation

The starting elements of the space-time aggregation process, are the discretized fields of rain accumulated over a time increment Δt = 5 min and averaged over a square-pixel of side length Δxy = 1 km. In the following, these rainfields are denoted as $r^*(x^*, y^*, t^*)$, where t^* is the ending time of the 5-min time-step, and $\{x^*, y^*\}$ is the center of the 1 km^2 pixel.

3.2.1 Spatial aggregation of 5 min rainfields

Let A be a surface over which the rainfall intensity is averaged. In this study, A is a square of side $Nx \times \Delta xy\ \mathrm{km} = Ny \times \Delta xy\ \mathrm{km}$ (corresponding to $Nx \times Ny$ pixels of 1 km^2). From the 5-min rainfields we can compute series of space averaged 5-min rainfield accumulations r^*_A, as:

$$r^*_A(x^*, y^*, t^*) = \frac{1}{A} \sum_{m=0}^{Nx-1} \sum_{n=0}^{Ny-1} r^* \left\{ x^* + \left(m - \frac{Nx-1}{2} \right) \Delta xy, y^* + \left(n - \frac{Ny-1}{2} \right) \Delta xy, t^* \right\}. \tag{18}$$

From these spatially averaged rainfields, spatial rainfall series have been extracted at rain-gauge locations. For each rain-gauge location (located at $\{x, y\}$), the nearest spatial rainfall

series r_A^* (located at $\{x^*, y^*\}$) is extracted. Figure 3a illustrates this approach (the black circle of the right panel represents a rain-gauge located at $\{x, y\}$. In total, 12 scales of spatial aggregations have been retained to build the rainfall series: $1\,\mathrm{km}^2$ (the pixel on which the station is located is selected) then 4, 9, 16, 25, 49, 100, 225, 400, 900, 1600 and $2500\,\mathrm{km}^2$.

To limit border effects, the spatial aggregation is performed only in areas where the spatial distribution of stations is more or less isotropic. Each of the 30 measurement stations is considered individually; a circle centered on the station is plotted and divided in eight cardinal sectors (each sector has an angle of 45 °). Only rain gauges having at least one other rain gauge present in at least seven of the eight sectors are retained for spatial aggregation (see Fig. 3a); the distance of the other gauges from the center station is not taken into account for the selection, only matters the presence or absence of a rain gauge in the sector. Only 13 gauges (out of 30) satisfy this criterion (Fig. 1). They are referred to in the following as central rain-gauges (CR) because their localization is used as a central point, from which the 12 areas of aggregation are delimited. In total there are thus 156 areal series (12 areas of aggregation centered on 13 different locations).

3.2.2 Time aggregation of 5-min point series and 5-min spatial series

A time aggregation procedure is applied to the 30 point 5-min rainfall series and to the 156 spatial rainfall series.

Let D be a given duration of Nt 5-min time-steps ($D = Nt \times \Delta t$). The time aggregation is done by using a moving time window of length D over which the 5-min rainfall intensity is averaged (this moving window procedure is carried out in order to make sure that we will be able to extract the maximum maximorum for each duration considered). The time aggregation can be written as:

$$r^*_{D,0}(x, y, t^*) = \frac{1}{D} \sum_{p=0}^{Nt-1} r^*_0(x, y, t^* - p \times \Delta t) \tag{19}$$

in the case of 5-min point series located at $\{x, y\}$ ($A = 0$), and

$$r^*_{D,A}(x^*, y^*, t^*) = \frac{1}{D} \sum_{p=0}^{Nt-1} r^*_A(x^*, y^*, t^* - p \times \Delta t) \tag{20}$$

for a given surface A in the case of 5-min spatial rainfall series located at $\{x^*, y^*\}$.

Thus, $Nt = 12$ for $D = 1\,\mathrm{h}$, $Nt = 24$ for $D = 2\,\mathrm{h}$ and so forth. This procedure is illustrated in Fig. 3b. The 11 different time resolutions considered in this study range from 1 to 24 h (1, 2, 3, 4, 6, 8, 10, 12, 15, 18 and 24 h) and are all obtained from the original 5-min series.

3.2.3 Extraction of extreme rainfall: annual block maxima

The use of GEV distribution to model the extreme rainfall series requires using the block maxima procedure to extract rainfall extremes. It consists of defining annual blocks of observations separately for each of the 11 different time resolutions considered and to take the maxima within each block. A sample of 23 (1990–2012) annual maximum rainfall values $\{i(D, A)\}$ is thus obtained for each spatial aggregation and duration.

In summary:

- there are 13 reference locations;
- around each of the 13 reference locations, 12 areas of increasing size 1, 4, 9, 16, 25, 49, 100, 225, 400, 900, 1600 and 2500 km^2 are defined;
- for each of these 156 (13×12) areas, 11 time series of 23 (1990–2012) annual maximum values are constructed, corresponding to 11 different durations of rainfall accumulation 1, 2, 3, 4, 6, 8, 10, 12, 15, 18, 24 h.

4 Inferences of the individual components of the model

The proposed model has seven parameters: the temporal scale exponent (η), the three ARF parameters (a, b, ω) and the three GEV parameters (μ_{ref}, σ_{ref}, ξ_{ref}). After having tested different optimization procedures (most notably a global maximum likelihood estimation and the 2-step method proposed by Koutsoyiannis et al., 1998) a 3-step method was finally retained, since it gave the best results in the evaluation of the IDAF model (see Sect. 5). These three steps are explained in the following paragraphs (Sects. 4.1 to 4.3). For each step, an illustration based on the result obtained for the Niamey Aéroport station is given in Fig. 4.

4.1 Temporal simple scaling: estimation of η

The temporal scaling of the IDAF model is described by the η parameter. The inference of η is achieved in two steps. The first one consists in computing $k(q)$ for different moments q through a linear regression between the logarithm of the statistical moments of order q ($E[I^q]$) and the durations D (see Fig. 4a, left panel). Then, η is obtained by a linear regression between $k(q)$ and q (see Fig. 4a, right panel). At the Niamey Aéroport station, the value obtained for η is equal to -0.91.

4.2 GEV parameters: μ_{ref}, σ_{ref}, ξ_{ref}

The GEV parameters μ_{ref}, σ_{ref}, ξ_{ref} are estimated on the point samples, using the property that all normalized samples $\{i(D,0)/D^{\eta}\}$ must come from the same distribution if simple scaling holds. All normalized samples are pooled in one single sample on which the GEV parameters are estimated (this methodology corresponds to the second step of the 2-step method proposed by Koutsoyiannis et al., 1998). Figure 4b illustrates this process at the Niamey Aéroport rain gauge: initial samples are displayed on the left panel, normalized samples are plotted on the right panel. The fitted GEV and the estimated GEV parameters are also given in this figure.

In comparison with fitting the GEV parameters separately to each sample constituted for each duration, this method aims at limiting sampling effects by fitting the GEV parameters on a single

sample gathering all rainfall durations. The maximum Likelihood and the L-Moments methods were tested for estimating the GEV parameters. The estimation provided by these methods gave similar results, probably due to the large sample size. The results of the L-Moments method are presented here, this method being generally considered better than the MLE for the estimation of high quantiles when the length of the series are short (Hosking and Wallis, 1997).

4.3 Spatial scaling

The estimation of a, b, ω was carried out by minimizing the mean square difference between the empirical ARF (Eq. 10) and the model ARF (Eq. 12), as originally proposed by De Michele et al. (2001). Other scores (mean and max absolute error, bias, ...) and variables (difference between the observed and model mean areal rainfall) have been tried but gave poorer results in validation (Sect. 5). Figure 4c shows the comparison between the empirical ARF and the model ARF at the Niamey Aéroport station and the parameters obtained for the theoretical ARF model.

4.4 Regional model

The point parameter inference (μ_{ref}, σ_{ref}, ξ_{ref} and η) has been performed on each of the 30 point rainfall series, which thus provide 30 IDF models. The complete IDAF model has been fitted to each of the 13 rain gauges CR. The obtained IDF and IDAF parameters do not display either any coherent spatial pattern or any trend over the domain, as may be seen in Figure 5. Sampling effects due to the small area and the short length of the series may explain this point, since a trend has been observed on a larger domain at the regional scale for daily rainfall (Panthou et al., 2012).

Assuming a spatial homogeneity of rainfall distribution (no spatial pattern), annual maxima series have been pooled together to obtain regional samples. The regional samples were used to fit the IDAF model over the domain in order to limit sampling effects. The point regional sample pools together the 30 rainfall samples directly provided by the 30 rain gauges $i(D, 0)$; the 12 areal regional samples obtained for each of the 12 spatial resolutions $\{i(D, A); A =$

$1, \ldots, 2500\,\mathrm{km}^2\}$ result from pooling together the 13 individual series (CR rain-gauges) computed as explained in Sect. 3.

Table 1 presents the parameters obtained for the global IDAF model. The obtained GEV parameters are μ_{ref}= 40.6 $\mathrm{mm\,h^{-1}}$, σ_{ref} = 10.8 $\mathrm{mm\,h^{-1}}$, and ξ_{ref} = 0.1. When upscaled to the daily duration μ(24 h) = 2.29 $\mathrm{mm\,h^{-1}}$ (55.0 $\mathrm{mm\,day^{-1}}$) and σ(24 h) = 0.61 $\mathrm{mm\,h^{-1}}$ (14.6 $\mathrm{mm\,day^{-1}}$). It is worth noting that these latter values are coherent with those obtained for a much larger area in this region by Panthou et al. (2012, 2013), working on the data of 126 daily rain gauges covering the period 1950-1990. Note also that the temporal scale exponent (η) is large (0.9), which means that the intensity strongly decreases as the duration increases. This is not surprising given the strong convective nature of rainfall in this region. Similar values of the temporal scaling exponents are obtained in regions where strong convective systems occur (Mohymont et al., 2004; Van-de Vyver and Demarée, 2010; Ceresetti et al., 2011) while lower values are obtained in regions where extreme rainfall is generated by different kinds of meteorological systems (for example in many mid-latitudes regions, see e.g. Menabde et al., 1999; Borga et al., 2005; Nhat et al., 2007). The dynamic scaling exponent is roughly equal to 1 which means that increasing the surface by a given factor leads to a similar ARF change than increasing the duration by the same factor (keeping in mind that this rule applies only to the range of time-space resolutions explored here).

5 IDAF model evaluation

The evaluation of the IDAF model is carried out in two successive stages. First each component used to build the final model (temporal simple scaling, ARF model and GEV distribution) is checked individually; then the global goodness of fit is tested using the Anderson–Darling (AD) and the Kolmogorov–Smirnov (KS) tests.

In Fig. 6 two series of graphs are plotted in order to verify whether the simple scaling hypothesis holds for the time dimension. On the left are the plots of $\ln(E[I^q])$ vs. $\ln(D)$ designed to check the log-log linearity between these two variables (Eq. 7); on the right are the plots of q vs. $k(q)$ aimed at checking the linearity between these two variables (Eq. 8). At all three spatial

scales, there is a clear linearity of the plots, meaning that the two conditions for accepting the temporal simple-scaling hypothesis are fulfilled. Note that the graphs shown are those obtained on the regional samples for 3 different spatial scales only (point scale, 100 and 2500 km^2), but the quality of the fitting is similar for all the other spatial scales.

Simple scaling in space and dynamical scaling (e.g. the relationship between time and spatial scaling) are checked in Fig. 7. This figure compares the empirical ARFs (Eq. 10) computed on the regional samples and the ARFs obtained with the model (Eq. 12) for all the space and time scales pooled together. With a determination coefficient (r^2) of 0.98, and a very small RMSE, it appears that the model restitutes very well the empirical ARF at all space and time scales, except at the hourly time step and for the three largest surfaces (900, 1600 and 2500 km^2), for which the model significantly underestimates the observed reduction factor. At such space–time scales the finite size of the convective systems generating the rain-fields creates a significant external intermittency (see Ali et al., 2003, on the distinction between internal and external intermittency). It thus seems that the simple scaling framework holds only as long as the influence of the external intermittency is negligible or weak. Consequently it is likely that the underestimation of the areal reduction factor by the simple scaling based model would be observed for larger space–time scales than the ones the AMMA-CATCH data set allows to explore.

Figure 8 illustrates that the global model is also able to reproduce very correctly the mean areal rainfall intensity over the whole time-space domain explored here, except again for the hourly time step and the largest surfaces.

As the IDAF model is primarily designed to estimate high quantiles, its ability to represent the mean is not a sufficient skill. It is thus of primary importance to evaluate its ability to also represent correctly high return levels and extreme quantiles. This was realized by visually inspecting return level plots and by using Goodness Of Fit (GOF) statistical tests computed in a cross validation mode (all the stations are used to calibrate the model except one which is used to validate the model prediction). These tests are used to quantitatively assess how well the theoretical GEV distribution based on the IDAF model fits the empirical CDFs of the observed annual maxima for each spatio-temporal resolution. Each test provides a statistic and

its corresponding p value. The p value is used as an acceptation/rejection criterion by fixing a threshold of non exceedance (here 1, 5, and 10 %).

The return level plots displayed in Fig. 9 for two reference locations and 3 time steps allow a visual inspection of the capacity of the global IDAF to fit the empirical samples. The p values of the two GOF tests are given in the inset caption. As could be expected, there is a significant dispersion of the results obtained on individual samples. The difficulty of reproducing correctly the empirical distribution when combining the smallest time steps with the largest areas is confirmed. While similar graphs were plotted for the other 11 reference locations, it is obviously difficult to obtain a relevant global evaluation from the visual examination of such plots.

Figure 10 aims at tackling this limitation by representing this information in a more synthetic way. In this figure the percentage of individual series for which the IDAF model is rejected by the Anderson–Darling GOF test is mapped for each duration and spatial aggregation for two levels of significance (1 and 10 %). Here it is worth remembering that we have 30 individual series for the point scale, and 13 different individual series for each of the 12 spatial scales, meaning that, for a given time step, the percentage of rejections/acceptations are computed from a total of 186 ($30 + 12 \times 13$) test values. Here again, the limits of the model for small time steps and large areas are clearly visible; one can also notice a larger number of rejections for small areas and the highest durations (duration higher than 12 h and area smaller than 25 km^2). Apart from that, the number of rejection of the null hypothesis remains low. The KS test (not shown) display similar result with a little less rejections of the null hypothesis. It thus appears fair to conclude that, over the range of space–time scales covered by the AMMA-CATCH network, a simple scaling approach allows for computing realistic areal reduction factors, the limit of validity being reached for areas roughly larger than 1000 km^2 at the hourly time step.

6 Discussion – conclusion

Up to now the rarity of rainfall measurements at high space–time resolution in Tropical Africa, had not permitted to carry out comprehensive studies on the scaling properties of rain-fields in that region. From 1990, the recording rain gauge network of the AMMA-CATCH observing

system samples rainfall in a typical Sahelian region of West Africa at a time resolution of 5 min and a space resolution of 20 km, over an area slightly larger than $1^\circ \times 1^\circ$. This data set was used here for characterizing the space–time structure of extreme rainfall distribution, the first time such an attempt is made in this region where rainfall is notoriously highly variable.

Simple scaling was shown to hold for both the time and the space dimensions over a space–time domain ranging from 1 to 24 h and from the point scale to 2500 km^2; it was further shown that dynamical scaling relates the time scales to the space scales, leading to propose a global IDAF model valid over this space–time domain, under the assumption that extreme rainfall values are GEV distributed.

Different optimization procedures were explored in order to infer the 7 parameters of this global IDAF model. A 3-step procedure was finally retained, the global IDAF model being fitted to a global sample built from all the different samples available for a given space–time scale. This model has been evaluated through different graphical methods and scores. These scores show that the areal reduction factors yielded by the IDAF model fit significantly well (in a statistical sense) the observed areal reduction factors over our space–time domain, except for the part of the domain combining the smallest time scales with the largest space scales. This limitation is likely related to the larger influence of the external intermittency of the rain-fields at such space–time scales.

Despite the growing accuracy of rainfall remote sensing devices, this study demonstrates that dense rain-gauge networks operating in a consistent way over long periods of time are still keys to the statistical modeling of extreme rainfall. In the numerous regions where rainfall is undersampled by operational networks and where satellite monitoring is not accurate enough to provide meaningful values of high rainfall at small space and time scales, dense networks covering a limited area may provide the information necessary for complementing the operational networks and satellite monitoring. In West Africa, south to the Niger site, AMMA-CATCH has been operating another site of similar size in a Soudanian climate since 1997 (Ouémé Catchment, Benin), providing ground for a similar study in a more humid tropical climate.

As mentioned in the discussion of Sect. 5, there is however a limitation of these two research networks, linked to their spatial coverage. Extending the area sampled by these networks to

something in the order of $2^\circ \times 2^\circ$ would indeed allow studying more finely the effect of the limited size of the convective systems onto the statistical properties of the associated rain-fields. However, this means enlarging the area by a factor 4, making it much more costly and difficult from a logistical point of view to survey properly. For the years to come, AMMA-CATCH remains committed to operating both the Niger and the Benin sites for documenting possible evolutions of the rainfall regimes at fine space and time scales in the context of global change as well as for verifying whether the scaling relationships proposed here still hold for quantiles at higher time periods. As a matter of fact, one strong hypothesis of the model proposed here is that the ARF is independent of the return period. This hypothesis seems verified for return periods smaller than the length of our time series, but it is not possible to infer whether this really holds for higher return periods. Therefore developing an IDAF model able to account for a possible evolution of the ARF with the return period level is a path that has to be explored, copulas being a candidate for such a development (e.g. Singh and Zhang, 2007; Ariff et al., 2012).

It is also envisioned to test other IDAF model formulations based on alternative approaches for modeling the scale relationships, among which the method proposed by Overeem et al. (2010) seems of particular interest.

Appendix A:

A brief explanation of the transition between the simple-scaling framework used to described the space–time scaling of maximum annual rainfall (Eq. 13) and the GEV model used to model the statistical distribution of these maxima (Eqs. 15 to 17) is given here.

The random variables $I(D_{\text{ref}}, 0)$ and $I(D, A)$ are modeled by a GEV model:

$$\text{Prob}\left\{I(D_{\text{ref}},0) \le i(D_{\text{ref}},0)\right\} = \exp\left\{-\left[1+\xi(D_{\text{ref}},0)\left(\frac{i(D_{\text{ref}},0)-\mu(D_{\text{ref}},0)}{\sigma(D_{\text{ref}},0)}\right)\right]^{-\frac{1}{\xi(D_{\text{ref}},0)}}\right\} \quad \text{(A1)}$$

and

$$\text{Prob}\{(I(D,A) \leq i(D,A)\} = \exp\left\{-\left[1+\xi(D,A)\left(\frac{i(D,A)-\mu(D,A)}{\sigma(D,A)}\right)\right]^{-\frac{1}{\xi(D,A)}}\right\}. \quad \text{(A2)}$$

Let introduce, $c = \lambda^{\eta} \times \text{ARF}(D,A)$ then Eq. (13) becomes:

$$I(D,A) \stackrel{d}{=} I(D_{\text{ref}},0) \times c \quad \text{(A3)}$$

and if Eq. (13) holds, then:

$$\begin{aligned}\text{Prob}\{I(D,A) \leq i(D,A)\} &= \text{Prob}\{I(D_{\text{ref}},0) \times c \leq i(D_{\text{ref}},0) \times c\} \\ &= \text{Prob}\{I(D_{\text{ref}},0) \leq i(D_{\text{ref}},0)\}\end{aligned} \quad \text{(A4)}$$

and

$$\text{Prob}\{I(D,A) \leq i(D,A)\} = \exp\left\{-\left[1+\xi(D_{\text{ref}},0)\left(\frac{i(D_{\text{ref}},0)-\mu(D_{\text{ref}},0)}{\sigma(D_{\text{ref}},0)}\right)\right]^{-\frac{1}{\xi(D_{\text{ref}},0)}}\right\}. \quad \text{(A5)}$$

By replacing $I(D_{\text{ref}},0)$ by $I(D,A)/c$ we obtain

$$\text{Prob}\{I(D,A) \leq i(D,A)\} = \exp\left\{-\left[1+\xi(D_{\text{ref}},0)\left(\frac{\frac{I(D,A)}{c}-\mu(D_{\text{ref}},0)}{\sigma(D_{\text{ref}},0)}\right)\right]^{-\frac{1}{\xi(D_{\text{ref}},0)}}\right\} \quad \text{(A6)}$$

or

$$\text{Prob}\{I(D,A) \leq i(D,A)\} = \exp\left\{-\left[1+\xi(D_{\text{ref}},0)\left(\frac{I(D,A)-\mu(D_{\text{ref}},0)\times c}{\sigma(D_{\text{ref}},0)\times c}\right)\right]^{-\frac{1}{\xi(D_{\text{ref}},0)}}\right\}.$$

(A7)

The equality between Eq. (A2) and Eq. (A7) gives:

$$\mu(D, A) = \mu_{\text{ref}} \times c \tag{A8}$$

$$\sigma(D, A) = \sigma_{\text{ref}} \times c \tag{A9}$$

$$\xi(D, A) = \xi_{\text{ref}}. \tag{A10}$$

Equations (A8) to (A10) correspond to Eqs. (15) to (17) in the main text.

Acknowledgements. This research was partly funded by the LABEX OSUG@2020 (ANR10 LABX56), partly by the French project ESCAPE (ANR10-CEPL-005), and partly by IRD and INSU through the support to the AMMA-CATCH observing system. Gérémy Panthou Ph.D. grant is funded by SOFRECO.

References

Ali, A., Lebel, T., and Amani, A.: Invariance in the Spatial Structure of Sahelian Rain Fields at Climatological Scales, Journal Of Hydrometeorology, 4, 996–1011, 2003.

Allen, R. and DeGaetano, A.: Areal Reduction Factors for Two eastern United States Regions with High Rain-Gauge Density, Journal of Hydrologic Engineering, 10, 327–335, 2005.

Ariff, N., Jemain, A., Ibrahim, K., and Wan Zin, W.: IDF relationships using bivariate copula for storm events in Peninsular Malaysia, Journal of Hydrology, 470-471, 158–171, 2012.

Asquith, W. H. and Famiglietti, J. S.: Precipitation areal-reduction factor estimation using an annual-maxima centered approach, Journal of Hydrology, 230, 55–69, 2000.

Awadallah, A.: Developing Intensity-Duration-Frequency Curves in Scarce Data Region: An Approach using Regional Analysis and Satellite Data, Engineering, 03, 215–226, 2011.

Bara, M., Kohnová, S., Gaál, L., Szolgay, J., and Hlavcová, K.: Estimation of IDF curves of extreme rainfall by simple scaling in Slovakia, Contributions to Geophysics and Geodesy, 39, 187–206, 2009.

Bell, F.: The areal reduction factor in rainfall frequency estimation, Tech. rep. 35, Institute of hydrology, Natural Environment Research Council, UK, 1976.

Ben-Zvi, A.: Rainfall intensity-duration-frequency relationships derived from large partial duration series, Journal of Hydrology, 367, 104–114, 2009.

Bendjoudi, H., Hubert, P., Schertzer, D., and Lovejoy, S.: Interprétation multifractale des courbes intensité-durée-fréquence des précipitations, C. R. Acad. Sci. Paris, Sciences de la terre et des planétes / Earth & Planetary Sciences, 325, 323–326, 1997.

Borga, M., Vezzani, C., and Fontana, G. D.: Regional rainfall depth-duration-frequency equations for an Alpine region, Natural Hazards, 36, 221–235, 2005.

Burlando, P. and Rosso, R.: Scaling and muitiscaling models of depth-duration-frequency curves for storm precipitation, Journal of Hydrology, 187, 45–64, 1996.

Castro, J. J., Cârsteanu, A. A., and Flores, C. G.: Intensity-duration-area-frequency functions for precipitation in a multifractal framework, Physica A: Statistical Mechanics and its Applications, 338, 206–210, 2004.

Ceresetti, D.: Structure spatio-temporelle des fortes précipitations: Application à la région Cévennes Vivarais, Ph.D. thesis, Université de Grenoble, 2011.

Ceresetti, D., Anquetin, S., Molinié, G., Leblois, E., and Creutin, J.: Multiscale Evaluation of Extreme Rainfall Event Predictions Using Severity Diagrams, Weather and Forecasting, 27, 174–188, 2011.

Coles, S.: An introduction to statistical modeling of extreme values, Springer, London;New York, 2001.

De Michele, C., Kottegoda, N. T., and Rosso, R.: The derivation of areal reduction factor of storm rainfall from its scaling properties, Water Resources Research, 37, 3247–3252, 2001.

De Michele, C., Kottegoda, N., and Rosso, R.: IDAF (intensity-duration-area frequency) curves of extreme storm rainfall: a scaling approach, Water science and technology, 45, 83–90, 2002.

De Michele, C., Zenoni, E., Pecora, S., and Rosso, R.: Analytical derivation of rain intensity-duration-area-frequency relationships from event maxima, Journal of Hydrology, 399, 385–393, 2011.

Descroix, L., Genthon, P., Amogu, O., Rajot, J. L., Sighomnou, D., and Vauclin, M.: Change in Sahelian Rivers hydrograph: The case of recent red floods of the Niger River in the Niamey region, Global and Planetary Change, 98-99, 18–30, 2012.

Di-Baldassarre, G., Montanari, A., Lins, H., Koutsoyiannis, D., Brandimarte, L., and Blöschl, G.: Flood fatalities in Africa: From diagnosis to mitigation, Geophysical Research Letters, 37, 1–5, 2010.

Gerold, L. and Watkins, D.: Short Duration Rainfall Frequency Analysis in Michigan Using Scale-Invariance Assumptions, Journal of Hydrologic Engineering, 10, 450–457, 2005.

Gupta, V. and Waymire, E.: Multiscaling properties of spatial rainfall and river flow distributions, Journal Of Geophysical Research, 95, 1999–2009, 1990.

Hosking, J. and Wallis, J. R.: Regional frequency analysis: an approach based on L-moments, Cambridge University Press, Cambridge UK, 1997.

Koutsoyiannis, D., Kozonis, D., and Manetas, A.: A mathematical framework for studying rainfall intensity-duration-frequency relationships, Journal of Hydrology, 206, 118–135, 1998.

Lebel, T., Sauvageot, H., Hoepffner, M., Desbois, M., Guillot, B., and Hubert, P.: Rainfall estimation in the Sahel: the EPSAT-NIGER experiment, Hydrological Sciences, 37, 201–215, 1992.

Menabde, M., Seed, A., and Pegram, G.: A simple scaling model for extreme rainfall, Water Resources Research, 35, 335–339, 1999.

Mohymont, B., Demarée, G. R., and Faka, D. N.: Establishment of IDF-curves for precipitation in the tropical area of Central Africa-comparison of techniques and results, Natural Hazards and Earth System Science, 4, 375–387, 2004.

Nhat, L., Tachikawa, Y., Sayama, T., and Takara, K.: A simple scaling charateristics of rainfall in time and space to derive intensity duration frequency relationships, Annual Journal of Hydraulic Engineering, 51, 73–78, 2007.

Overeem, A., Buishand, A., and Holleman, I.: Rainfall depth-duration-frequency curves and their uncertainties, Journal Of Hydrology, 348, 124–134, 2008.

Overeem, A., Buishand, T. A., and Holleman, I.: Extreme rainfall analysis and estimation of depth-duration-frequency curves using weather radar, Water Resources Research, 45, W10 424, 2009.

Overeem, A., Buishand, T. A., Holleman, I., and Uijlenhoet, R.: Extreme value modeling of areal rainfall from weather radar, Water Resources Research, 46, W09 514, 2010.

Oyebande, L.: Deriving rainfall intensity-duration-frequency relationships and estimates for regions with inadequate data, Hydrol. Sci. J, 27, 353–367, 1982.

Oyegoke, S. and Oyebande, L.: A new technique for analysis of extreme rainfall for Nigeria, Environmental Research Journal, 2, 7–14, 2008.

Panthou, G., Vischel, T., Lebel, T., Blanchet, J., Quantin, G., and Ali, A.: Extreme rainfall in West Africa: A regional modeling, Water Resources Research, 48, 1–19, 2012.

Panthou, G., Vischel, T., Lebel, T., Quantin, G., Pugin, A.-C., Blanchet, J., and Ali, A.: From pointwise testing to a regional vision: An integrated statistical approach to detect nonstationarity in extreme daily rainfall. Application to the Sahelian region, Journal of Geophysical Research: Atmospheres, 118, 8222–8237, 2013.

Papalexiou, S. and Koutsoyiannis, D.: Battle of extreme value distributions: A global survey on extreme daily rainfall, Water Resources Research, 49, 187–201, 2013.

Ribstein, P. and Rodier, J.: La predetermination des crues sur des petits bassins saheliens inferieurs à 10 km2, Tech. rep., ORSTOM, Laboratoire d'hydrologie, Montpellier, 1994.

Rodier, J. and Ribstein, P.: Estimation des caracteristiques de la crue decennale pour les petits basins versants du Sahel couvrant de 1 a 10 km2, Tech. rep., ORSTOM, Laboratoire d'hydrologie, Montpellier, 1988.

Samimi, C., Fink, A., and Paeth, H.: The 2007 flood in the Sahel: Causes, characteristics and its presentation in the media and FEWS NET, Natural Hazards and Earth System Sciences, 12, 313–325, 2012.

Schertzer, D. and Lovejoy, S.: Physical Modeling and Analysis of Rain and Clouds by Anisotropic Scaling Multiplicative Processes, Journal of Geophysical Research, 92, 9693–9714, 1987.

Singh, V. and Zhang, L.: IDF Curves Using the Frank Archimedean Copula, Journal of Hydrologic Engineering, 12, 651–662, 2007.

Soro, G., Goula, B. T. A., Kouassi, F., and Srohourou, B.: Update of Intensity-Duration-Frequency curves for precipitation of short durations in tropical area of West Africa (cote d'Ivoire), Journal Of Applied Sciences, 10, 704–715, 2010.

Tarhule, A.: Damaging Rainfall and Flooding: The Other Sahel Hazards, Climatic Change, 72, 355–377, 2005.

Van-de Vyver, H. and Demarée, G. R.: Construction of Intensity-Duration-Frequency (IDF) curves for precipitation at Lubumbashi, Congo, under the hypothesis of inadequate data, Hydrological Sciences Journal-Journal des Sciences Hydrologiques, 55, 555–564, 2010.

Veneziano, D., Furcolo, P., and Iacobellis, V.: Imperfect scaling of time and space-time rainfall, Journal of Hydrology, 322, 105–119, 2006.

Vischel, T., Quantin, G., Lebel, T., Viarre, J., Gosset, M., Cazenave, F., and Panthou, G.: Generation of High-Resolution Rain Fields in West Africa: Evaluation of Dynamic Interpolation Methods, Journal of Hydrometeorology, 12, 1465–1482, 2011.

Yu, P., Yang, T., and Lin, C.: Regional rainfall intensity formulas based on scaling property of rainfall, Journal of Hydrology, 295, 108–123, 2004.

Table 1. Obtained parameters for the global IDAF model (a) and corresponding GEV parameters values for the different durations D for the point scale A=0 (b)

μ_{ref}	σ_{ref}	xi	η	a	b	z	ω
40.60	10.81	0.10	-0.90	0.165	0.156	1.06	0.026

(a)

GEV Parameter	1h	2h	3h	4h	6h	8h	10h	12h	15h	18h	24h
μ (mm h^{-1})	40.60	21.68	15.02	11.58	8.02	6.19	5.05	4.29	3.50	2.97	2.29
σ (mm h^{-1})	10.81	5.77	4.00	3.08	2.14	1.65	1.35	1.14	0.93	0.79	0.61
ξ (-)	0.10										

(b)

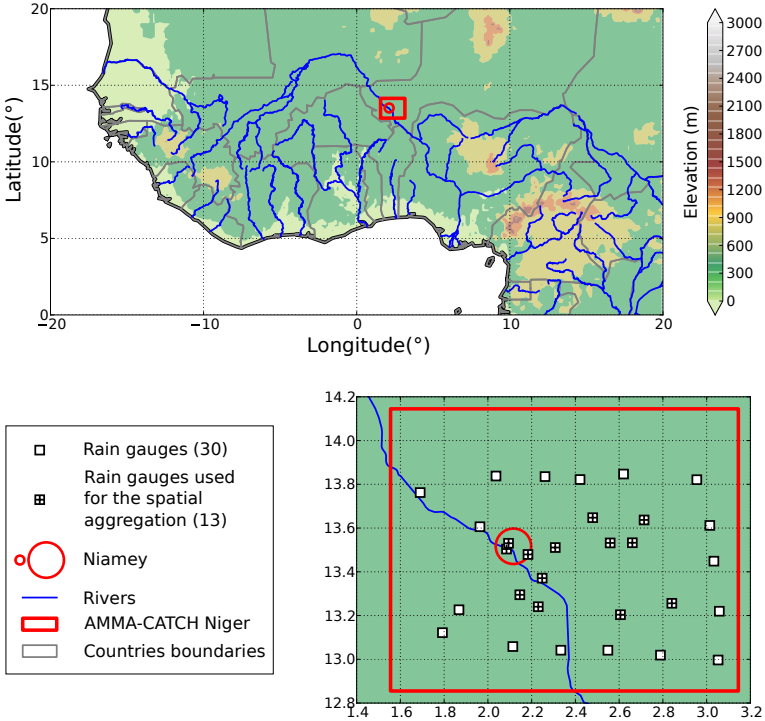

Figure 1. Study area. The background maps displays the elevation (meters).

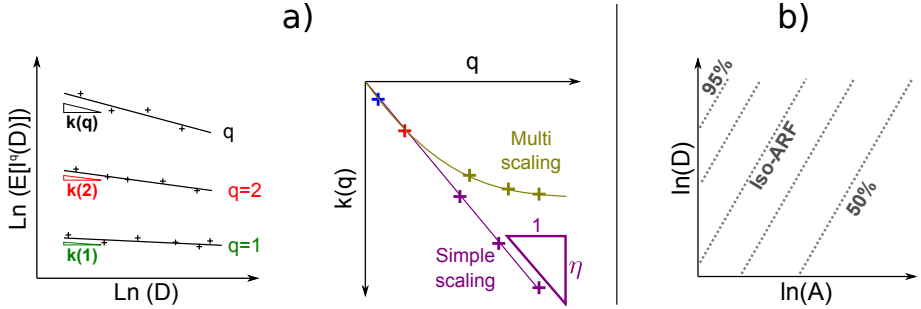

Figure 2. Visual model checks: **(a)** simple scaling; **(b)** ARF.

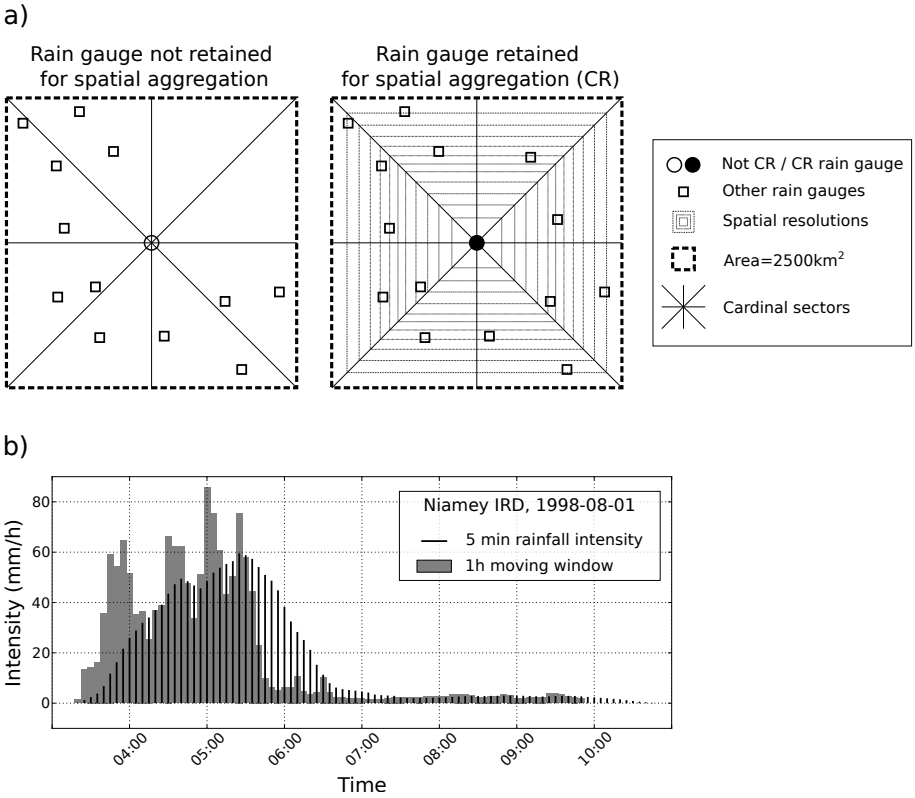

Figure 3. Examples of space and time aggregation used: **(a)** spatial aggregation, **(b)** time aggregation.

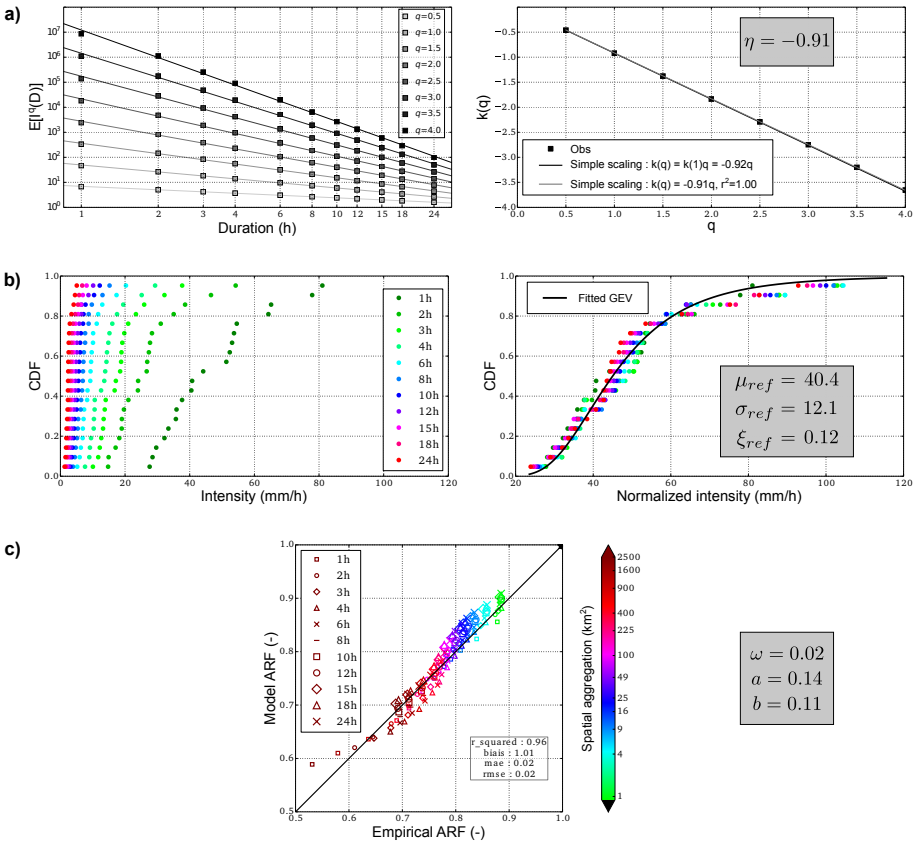

Figure 4. Example of IDAF model inference at the Niamey Aeroport rain gauge: **(a)** Checking of the temporal simple scaling conditions (left: linear relationship between the logarithm of the statistical moments of order q and the durations D, right: linear relationship between $k(q)$ and q) and estimation of the temporal simple scaling exponent; **(b)** left: empirical cumulative distribution of annual maxima, right: global fitting of the GEV parameters; **(c)** Comparison between empirical and modelled ARF.

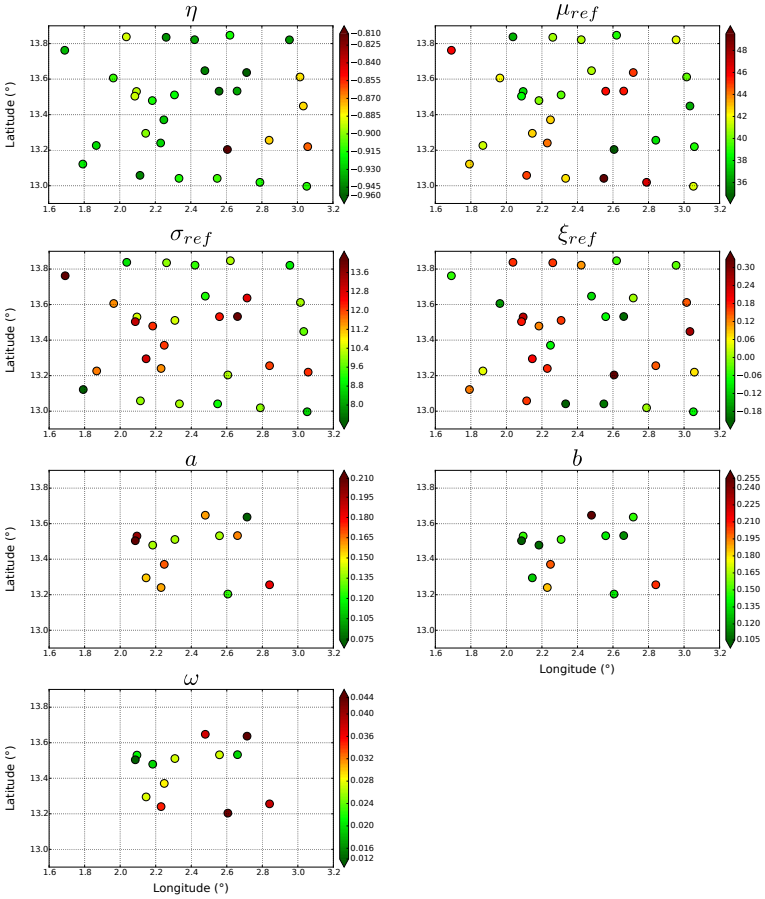

Figure 5. Map of the obtained IDF parameters (η, μ_{ref}, σ_{ref} and ξ_{ref} fitted on the 30 rain gauges samples) and IDAF parameters (η, μ_{ref}, σ_{ref}, ξ_{ref}, a, b and ω fitted on the 13 CR rain gauge samples).

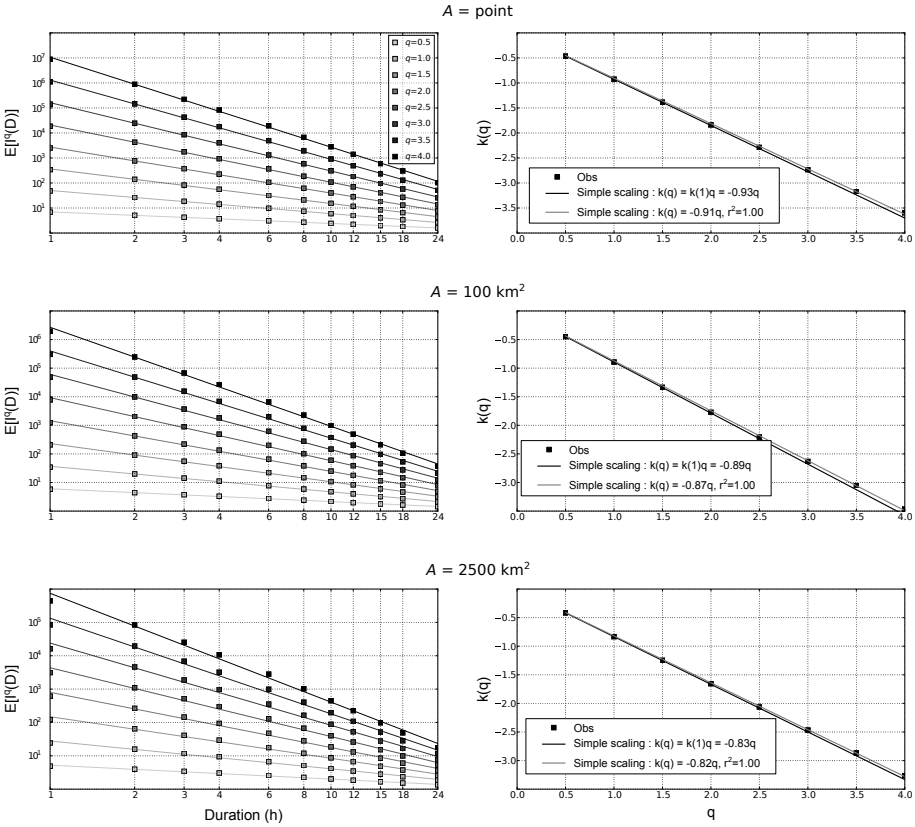

Figure 6. Checking of the temporal simple scaling conditions for the regional samples defined by the 30 available rain gauges for point resolution (top), and the 13 CR rain gauges (see Section 3.2.1) for the resolutions 100 km^2 (middle) and 2500 km^2 (bottom).

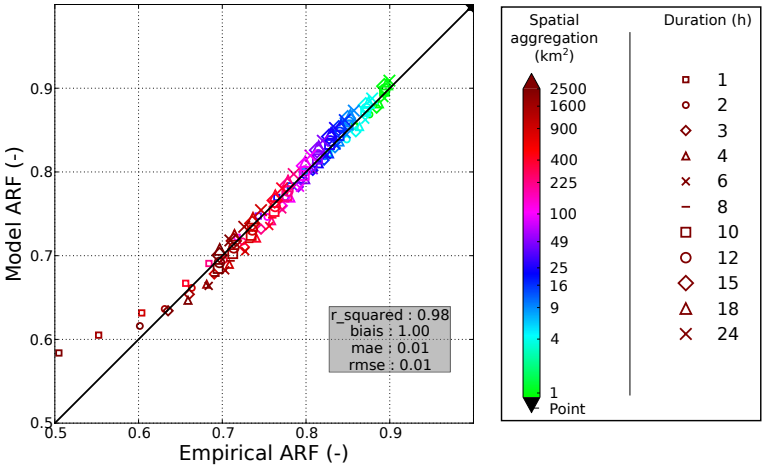

Figure 7. Comparison between empirical ARF (obtained with the regional samples: 30 rain gauges for point resolution and 13 CR rain gauges for other spatial resolutions) and modelled ARF IDAF model.

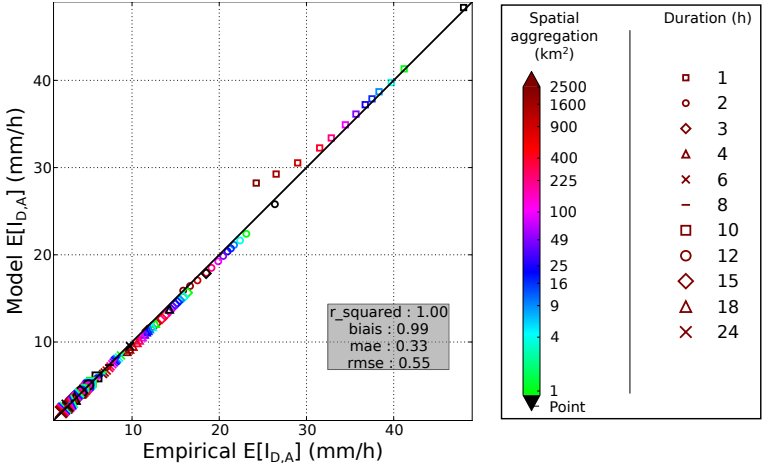

Figure 8. Comparison between empirical mean areal rainfall intensity (obtained with the regional samples: 30 rain gauges for point resolution and 13 CR rain gauges for other spatial resolutions) and global IDAF model for different spatio-temporal aggregations.

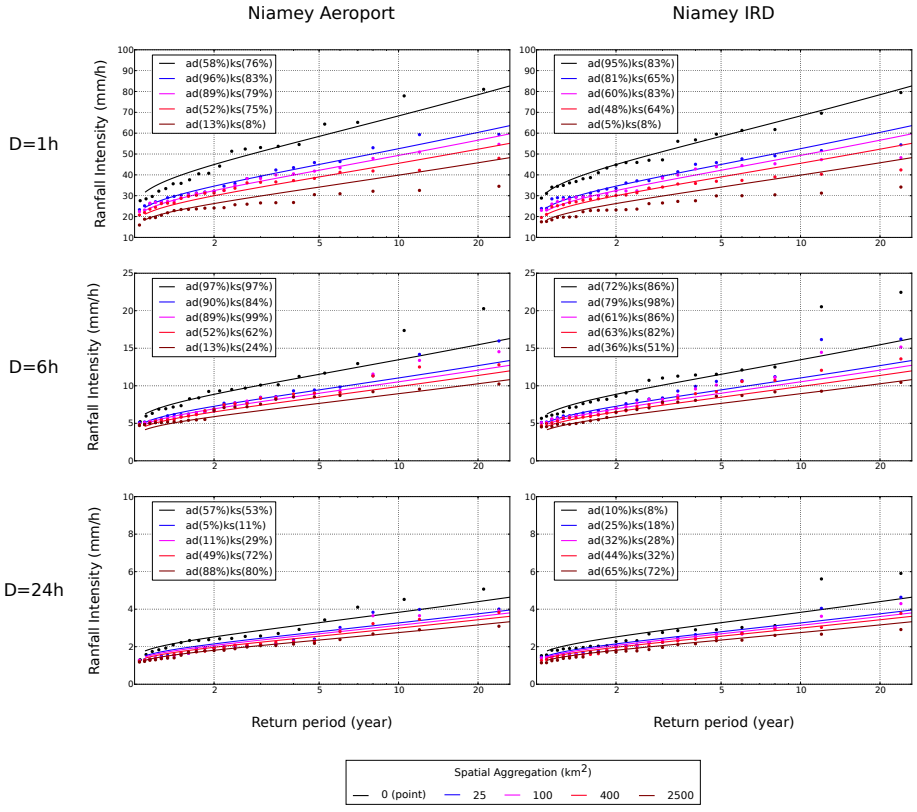

Figure 9. Empirical return level plot obtained at two rain gauges in comparison with the global IDAF model for different durations (1 h, 6 h and 24 h from top to bottom) and different spatial aggregations (from point to 2500 km^2).

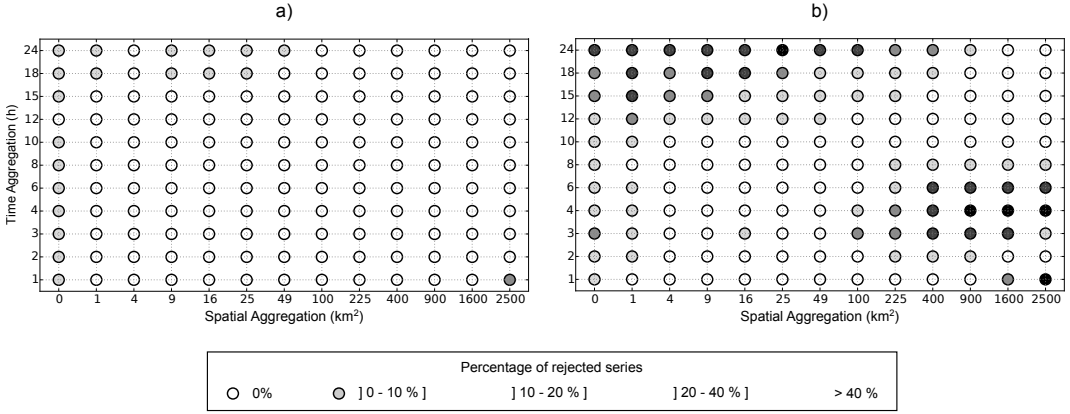

Figure 10. Anderson–Darling GOF test (cross validation): Percentage of rejected series for 1 % **(a)** and 10 % **(b)** significance level for the global IDAF model. Note that there are 30 series for the point scale ($0\,\mathrm{km}^2$) and 13 for the other spatial aggregation (rain gauges CR).

Manuscript prepared for Hydrol. Earth Syst. Sci. Discuss.
with version 2014/05/30 6.91 Copernicus papers of the LaTeX class copernicus.cls.
Date: 17 October 2014

Characterizing the space–time structure of rainfall in the Sahel with a view to estimating IDAF curves

G. Panthou, T. Vischel, T. Lebel, G. Quantin, and G. Molinié

LTHE – UMR5564, Univ. Grenoble, IRD, CNRS, Grenoble, France

Correspondence to: T. Vischel (theo.vischel@ujf-grenoble.fr)

Abstract

Intensity–duration–area–frequency (IDAF) curves are increasingly demanded for characterizing the severity of storms and for designing hydraulic structures. Their computation requires inferring areal rainfall distributions over the range of space–time scales that are the most relevant for hydrological studies at catchment scale. In this study, IDAF curves are computed for the first time in West Africa, based on the data provided by the AMMA-CATCH Niger network, composed of 30 recording rain gauges having operated since 1990 over a 16 000 km^2 area in South West Niger. The IDAF curves are obtained by separately considering the time (IDF) and space (Areal Reduction Factor – ARF) components of the extreme rainfall distribution. Annual maximum intensities are extracted for resolutions between 1 and 24 h in time and from point (rain-gauge) to 2500 km^2 in space. The IDF model used is based on the concept of scale invariance (simple scaling) which allows the normalization of the different temporal resolutions of maxima series to which a global GEV is fitted. This parsimonious framework allows using the concept of dynamic scaling to describe the ARF. The results show that coupling a simple scaling in space and time with a dynamical scaling relating space and time allows modeling satisfactorily the effect of space–time aggregation on the distribution of extreme rainfall.

1 Introduction

Torrential rain and floods have long been a major issue for hydrologists. For one, defining and computing their probability of occurrence is a scientific challenge *per se*, largely because it is a scale-dependent exercise. Secondly, and as important, is the fact that they cause heavy environmental, societal, and economical damages – including human losses – thus being a major concern for populations and decision makers.

The request of providing both an objective assessment of the probability of occurrence of high impact rainfall and a tool for civil engineering structure design has found an answer through the calculation of intensity–duration–frequency (IDF) curves. These curves, generally computed from rain gauge data, are intended at characterizing the evolution of extreme rainfall distribu-

tions at a point when the duration of rainfall accumulation changes. However rainfall at point location is not of greatest interest when it comes to the hydrological and socio-economic impacts of extreme events, since it is essentially the convolution of the rainfall intensities over a catchment that characterizes the severity of storms and creates the real threat.

This is why intensity–duration–area–frequency (IDAF) curves were conceived as a spatial extension of the IDF curves. Generally established by combining IDF curves and Areal Reduction Factors (ARF), they provide an estimation of extreme areal rainfall quantiles over a range of time and spatial scales.

Theoretical studies on IDF and ARF have been an active research topic over the past 20 years or so (Koutsoyiannis et al., 1998; Menabde et al., 1999; De Michele et al., 2001, 2011, among others). IDF practical studies are also numerous but focused on regions where long series of sub-daily rainfall are available (e.g. Borga et al., 2005; Gerold and Watkins, 2005; Nhat et al., 2007; Bara et al., 2009; Ben-Zvi, 2009; Overeem et al., 2009; Awadallah, 2011; Ariff et al., 2012) . On the other hand, when ARF are computed from rain gauge networks (Bell, 1976; Asquith and Famiglietti, 2000; Allen and DeGaetano, 2005), it requires a fair density of rain gauges in order to obtain accurate estimates of areal rainfall. The computation of IDAF curves must therefore deal with two major data requirements: (i) a high density network of rain gauges having produced and (ii) an array of long subdaily rainfall series. In addition to these requirements, scientists face the challenge of producing coherent ARF and IDF models, if they wish their IDAF model to be statistically consistent. This explains why there are so few studies dealing with the implementation of an IDAF model over a given region (e.g. De Michele et al., 2002; Castro et al., 2004; De Michele et al., 2011; Ceresetti, 2011) .

In fact, in some regions of the world there are virtually no IDF, ARF and IDAF models that have ever been conceived because of data limitations. This is especially the case in many tropical regions, such as West Africa, one reason being that a harsh environment and resource scarcity have make very challenging the operation of recording rain gauge networks. The few IDF studies available in the region (Oyebande, 1982; Mohymont et al., 2004; Oyegoke and Oyebande, 2008; Soro et al., 2010) are essentially empirical with no theoretical background allowing to upgrade their results in order to produce IDAF curves. ARF studies are still fewer,

the most noticeable being an attempt by Rodier and Ribstein (1988) and Ribstein and Rodier (1994) at computing ARF values for a return period of 10 years, with no explicit inference of the areal rainfall distributions. All in all, there has never been any IDAF model derived for West Africa or sub-regions of West Africa. Yet, flood management – for which IDAF curves are a very useful tool – is now a major concern for West African countries. As a matter of fact and despite that West Africa is known for having experienced a major lasting drought over 1970–2000, numerous severe floods and exceptional inundations have struck the region over the last two decades (Tarhule, 2005; Descroix et al., 2012; Samimi et al., 2012). Moreover, the flood damages in the region have been in constant increase since 1950 (Di-Baldassarre et al., 2010).

While operational networks of the West African National Weather Services do not allow the establishment of IDAF curves in a consistent way – because they do not provide any long term subdaily rainfall series – there are other sources of data that can be used for that purpose. Among them are the 5-min rainfall series of the long term AMMA-CATCH observing system covering a 16 000 km^2 area in South West Niger from 1990 onwards (Fig. 1). In this study we will make use of 30 series providing continuous 5-min rainfall records from 1990 to 2012.

This unique data set enables us to characterize the relationship between extreme rainfall distributions computed at various spatio-temporal scales and to propose IDAF curves for this characteristic Sahelian region.

2 IDAF curves in a GEV distribution and scale invariance framework

IDAF curves are providing an estimate of areal rain-rates – averaged over a given duration D and a given area A – for a given frequency of occurrence (currently expressed in term of return period T_r). In practice, IDAF curves are generally obtained by aggregating a temporal component and a spatial component represented respectively by the intensity–duration–frequency curves (IDF) computed at a point ($A = 0$) and by the Areal Reduction Factors (ARF) computed for a range of duration. In this framework, the most general formulation of an IDAF equation is as follows:

$$\mathrm{IDAF}(D, A, T_\mathrm{r}) = \mathrm{IDF}(D, T_\mathrm{r}) \times \mathrm{ARF}(D, A, T_\mathrm{r}). \quad (1)$$

Assessing IDAF curves requires: (i) inferring appropriate statistical distributions of rainfall to estimate the return periods and (ii) describing the statistical links between the distributions obtained at different space–time scales.

Several recent studies have confirmed that the Generalized Extreme Value (GEV) distribution (Coles, 2001) provides a suitable framework to describe the distribution of extreme rainfall at a point (e.g. Overeem et al., 2008; Panthou et al., 2012; Papalexiou and Koutsoyiannis, 2013). Also, many authors have shown that rainfall displays scale invariance properties (Schertzer and Lovejoy, 1987; Gupta and Waymire, 1990; Burlando and Rosso, 1996; Bendjoudi et al., 1997; Veneziano et al., 2006); both in space and time. The temporal scaling properties give access to a direct analytical formulation of IDF curves (Menabde et al., 1999; Borga et al., 2005; Ceresetti, 2011), while the spatial scaling properties allow to upscale IDF curves into IDAF curves (De Michele et al., 2002; Castro et al., 2004; De Michele et al., 2011) , thus providing an integrated space–time characterization of extreme rainfall distributions. Under certain assumptions, namely the GEV distribution of point annual rainfall maxima and simple scaling in both time and space, an analytical formulations of the various components of Eq. (1) may be obtained, as will be detailed below.

2.1 GEV distribution

Let us define $I(D,A)$ a random variable representing the annual maxima of rainfall accumulated over a given duration D and area A, and $i(D,A)$ a sample of $I(D,A)$. In the general framework of the block maxima sampling scheme (Coles, 2001), working on annual maxima generally ensures that the block size is large enough for the maxima distribution to follow a GEV distribution (Coles, 2001), written as:

$$G(i;\mu,\sigma,\xi) = \exp\left\{-\left[1+\xi\left(\frac{i-\mu}{\sigma}\right)\right]^{-\frac{1}{\xi}}\right\} \quad \text{for } 1+\xi\left(\frac{i-\mu}{\sigma}\right) > 0 \tag{2}$$

where i is a generic notation for any value associated with a realization of $I(D,A)$, μ being the location parameter, $\sigma > 0$ the scale parameter and ξ the shape parameter of the GEV distribution. The shape parameter describes the behavior of the distribution tail: a positive (resp.

negative) shape corresponds to a heavy tailed (resp. bounded) distribution. When ξ is equal to 0, the GEV reduces to the Gumbel distribution (light tailed distribution):

$$G(zi;\mu,\sigma) = \exp\left\{-\exp\left[-\left(\frac{i-\mu}{\sigma}\right)\right]\right\}. \tag{3}$$

2.2 Simple scaling in time and analytical formulation of IDF curves

The simple scaling framework has been extensively used for deriving IDF curves (Menabde et al., 1999; Yu et al., 2004; Borga et al., 2005; Nhat et al., 2007; Bara et al., 2009; Ceresetti, 2011). It provides a much more tractable analytical framework than the multi-scaling approach and is more robust in terms of parameter inference.

The annual maximum point rainfall random variable ~~{~~$I(D,0)$~~}~~ follows a simple scaling relation for a given duration D – with respect to a reference duration D_{ref} – if:

$$I(D,0) \overset{d}{=} \lambda^{\eta} \times I(D_{\text{ref}},0) \tag{4}$$

where λ is a scale ratio ($\lambda = D/D_{\text{ref}}$), η is a scale exponent and $\overset{d}{=}$ denotes an equality in distribution. Note that, for every duration D for which Eq. (4) holds, the normalized random variable ~~{~~$I(D,0)/D^{\eta}$~~}~~ has the same statistical distribution than the normalized reference distribution ~~{~~$I(D_{\text{ref}},0)/D_{\text{ref}}^{\eta}$~~}~~; this property will be used in the optimization procedure, in Sect. 4.2. Equation (4) implies (Gupta and Waymire, 1990):

$$E[I(D,0)] = \lambda^{\eta} \times E[I(D_{\text{ref}},0)] \tag{5}$$

and, more generally, a scaling of all the moments, that can be written as:

$$E[I^q(D,0)] = \lambda^{k(q)} \times E\left[I^q(D_{\text{ref}},0)\right]. \tag{6}$$

Or:

$$\ln\{E[I^q(D,0)]\} = k(q)\ln(\lambda) + \ln\left\{E\left[I^q(D_{\text{ref}},0)\right]\right\}. \tag{7}$$

The notion of simple scaling is related to how $k(q)$ evolves with q. When this evolution is linear:

$$k(q) = \eta q \tag{8}$$

then simple scaling holds (as opposed to multi-scaling if this relation in non linear).

Checking whether the simple scaling hypothesis is admissible over a given range of durations is thus equivalent to verifying on the data set whether the two following conditions are fulfilled (Gupta and Waymire, 1990):

- Eq. (7): log–log linearity between the statistical moments of any given order q;
- Eq. (8): linearity between $k(q)$ and q, $\eta(= k(1))$ being the scaling factor at order 1.

Figure 2a illustrates these two conditions.

2.3 Spatial scaling, dynamical scaling and ARF model

In its most general sense, the Areal Reduction Factor is the ratio between point rainfall and areal rainfall, either for a given observed rain event or in a statistical sense. Here we are interested in deriving a statistical ARF that can be used for obtaining an analytical formulation of IDAF curves (which implies that the ARF does not depend on the return period considered); this ARF thus denotes the ratio between the point distribution and the areal distribution of the annual rainfall maxima:

$$I(D,A) \stackrel{d}{=} \mathrm{ARF}(D,A) \times I(D,0). \tag{9}$$

Note that Eq. (9) implies the following relationship:

$$\mathrm{ARF}(D,A) = \frac{E[I(D,A)]}{E[I(D,0)]}. \tag{10}$$

In this study, the ARF model proposed by De Michele et al. (2001) is used. This model is based on two assumptions (which will have to be verified, see Sect. 5):

1. the studied rainfall variable is characterized by a simple scaling relationship both in time and space;

2. time and spatial scales are linked by a so-called dynamic scaling property written as:

$$\left(\frac{D}{D_{\text{ref}}}\right) = \left(\frac{A}{A_{\text{ref}}}\right)^{z} \tag{11}$$

where z is the dynamical scaling exponent.

When these assumptions are verified, De Michele et al. (2001) show that the ARF can be written as:

$$\text{ARF}(D, A) = \left[1 + \omega\left(\frac{A^a}{D^b}\right)\right]^{\eta/b} = \left[1 + \omega\left(\frac{A^z}{D}\right)^b\right]^{\eta/b} \tag{12}$$

where:

- η is the scaling exponent characterising the temporal simple scaling;
- a and b are two positive constant scaling exponents linked by the relation $z = a/b$;
- ω is a factor of normalization.

This ARF formulation implies that iso-ARF are lines in the plane ~~$\ln(A), \ln(D)$~~ $\{\ln(A), \ln(D)\}$ as shown in Fig. 2b (De Michele et al., 2001).

2.4 GEV simple scaling IDAF model

By assuming that the maximum annual rainfall is GEV-distributed and that the scaling relations in time and space (Sects. 2.2 and 2.3) are verified, then the IDAF model is:

$$I(D, A) \stackrel{d}{=} I(D_{\text{ref}}, 0) \times \lambda^{\eta} \times \text{ARF}(D, A). \tag{13}$$

As shown in the Appendix A, the compatibility of the simple scaling and GEV frameworks is defined by the following equations:

$$I(D,A) \sim \mathrm{GEV}\left\{\left\{\mu(D,A), \sigma(D,A), \xi(D,A)\right\}\right\} \tag{14}$$

$$\mu(D,A) = \mu_{\mathrm{ref}} \times D^{\eta} \times \mathrm{ARF}(D,A) \tag{15}$$

$$\sigma(D,A) = \sigma_{\mathrm{ref}} \times D^{\eta} \times \mathrm{ARF}(D,A) \tag{16}$$

$$\xi(D,A) = \xi_{\mathrm{ref}}. \tag{17}$$

where μ_{ref}, σ_{ref} , and ξ_{ref} correspond to the GEV parameters computed for the arbitrary reference duration D_{ref}.

3 Data and implementation

Rainfall observing systems usually do not provide direct measurements at all the space and time scales required for an IDAF study; it is thus needed to derive from the ~~initial~~ raw data set, an elaborated data set that will allow verifying the various assumptions founding the theoretical framework defined in Sect. 2.

Accordingly, this section describes both the rainfall samples initially available on our Sahelian region of South-West Niger and the process used to obtain the final data set from which the IDAF curves were computed. This process consists in two major steps:

1. Space–time aggregation of the ~~initial~~ 5-min point rain-rates in order to obtain the average rain-rates for various space (A) and time (D) resolutions;
2. Extraction of extreme rainfall samples for each of the above resolutions.

3.1 The ~~initial~~ rainfall data set: AMMA-CATCH Niger records

The AMMA-CATCH Niger observing system was set up at the end of the 1980s as part of the long term monitoring component of the Hapex-Sahel experiment (Lebel et al., 1992). Since

then, it has operated continuously a large array of meteorological and hydrological instruments, providing a unique set of high resolution hydrometeorological data, covering a 16 000 km^2 area in South West Niger. For the purpose of this research, a subset of 30 5-min rainfall series was selected (Fig. 1), covering the entire 1990–2012 period. At each station, all year with more than 25 % of missing data have been removed in order to limit any sampling effect due to missing data in a particular year. After this quality control, all stations remain with at least 20 years of valid data, constituting our ~~initial~~ raw data sample.

To estimate areal rainfall intensities, this study makes use of the dynamical kriging interpolation method proposed by Vischel et al. (2011). Rainfields are produced over the domain of study at a time resolution of 5 min and a spatial resolution of 1 km^2.

3.2 Space–time rainfall aggregation

~~Hereafter, we denote by $r(x,y,t)$ the actual~~ The starting elements of the space-time aggregation process, are the discretized fields of rain accumulated over a time increment Δt = 5 min and averaged over a square-pixel of side length Δxy = 1 km. In the following, these rainfields are denoted as $r^*(x^*,y^*,t^*)$, where t^* is the ending time of the 5-min ~~rainfall accumulation recorded at a given time t and at a given rain gauge of coordinates (x,y).~~ time-step, and $\{x^*,y^*\}$ is the center of the 1 km^2 pixel.

3.2.1 Spatial aggregation of 5 min rainfields

Let A be a surface over which the rainfall intensity is averaged. In this study, A is a square of side ~~$2\Delta x = 2\Delta y$~~ $Nx \times \Delta xy$ km $= Ny \times \Delta xy$ km (corresponding to $Nx \times Ny$ pixels of 1 km^2). From the 5-min rainfields we can compute series of space averaged 5-min ~~rainfall intensities r_A~~ rainfield accumulations r^*_A, as:

$$r_A(x,y,t) = \frac{1}{A} \int_{x-\Delta x}^{x+\Delta x} \int_{y-\Delta y}^{y+\Delta y} r(x,y,t)\mathrm{d}x\mathrm{d}y.$$

~~These~~

$$r_A^*(x^*,y^*,t^*) = \frac{1}{A}\sum_{m=0}^{Nx-1}\sum_{n=0}^{Ny-1} r^*\left\{x^* + \left(m - \frac{Nx-1}{2}\right)\Delta xy, y^* + \left(n - \frac{Ny-1}{2}\right)\Delta xy, t^*\right\}. \quad (18)$$

From these spatially averaged rainfields, spatial rainfall series have been ~~computed~~ extracted at rain-gauge locations~~, meaning that $\{x,y\}$ in Eq. (18)correspond to the localization of the point series ($A = 0$)~~. For each rain-gauge location (located at $\{x,y\}$), the nearest spatial rainfall series r_A^* (located at $\{x^*,y^*\}$) is extracted. Figure 3a illustrates this approach (~~A0~~ the black circle of the right panel represents a rain-gauge located at $\{x,y\}$). In total, 12 scales of spatial aggregations have been retained to build the rainfall series: 1 km^2 (the pixel on which the station is located is selected) then 4, 9, 16, 25, 49, 100, 225, 400, 900, 1600 and 2500 km^2.

To limit border effects, the spatial aggregation is performed only ~~at reference stations surrounded by a sufficient number of rain gauges. To select these reference stations , a~~ in areas where the spatial distribution of stations is more or less isotropic. Each of the 30 measurement stations is considered individually; a circle centered on ~~each rain gauge~~ the station is plotted and divided in eight cardinal sectors (each sector has an angle of 45 °). Only rain gauges having at least one other rain gauge present in at least seven of the eight sectors are retained for spatial aggregation ~~. This leads to retain~~ (see Fig. 3a); the distance of the other gauges from the center station is not taken into account for the selection, only matters the presence or absence of a rain gauge in the sector. Only 13 gauges (out of 30) ~~such rain gauges~~ satisfy this criterion (Fig. 1). ~~The localization of each of these~~ They are referred to in the following as central rain-gauges ~~is a~~ (CR) because their localization is used as a central point, from which the 12 areas of aggregation are ~~defined. In the latter, these rain gauges will be denoted CR (central rain-gauges). In~~ delimited. In total there are thus 156 areal series (12 areas of aggregation ~~defined from~~ centered on 13 different locations).

3.2.2 Time aggregation of 5-min point series and 5-min spatial series

A time aggregation procedure is applied to the 30 point 5-min rainfall series and to the 156 spatial rainfall series.

Let D be a given duration of Nt 5-min time-steps ($D = Nt \times \Delta t$). The time aggregation is done by using a moving time window of length D over which the 5-min rainfall intensity is averaged (this moving window procedure is carried out in order to make sure that we will be able to extract the maximum maximorum for each duration considered). ~~For a given surface A, the~~ The time aggregation can be written as:

$$r_{D,A}(x,y,t) = \frac{1}{D}\int_{t-D}^{t} r_A(x,y,t)\mathrm{d}t.$$

~~Since r is discretized (~~

$$r^*_{D,0}(x,y,t^*) = \frac{1}{D}\sum_{p=0}^{Nt-1} r^*_0(x,y,t^* - p\times\Delta t) \quad (19)$$

in the case of 5-min ~~interval), D corresponds to the number of time-steps aggregated: 12 time-steps are considered~~ point series located at $\{x,y\}$ ($A = 0$), and

$$r^*_{D,A}(x^*,y^*,t^*) = \frac{1}{D}\sum_{p=0}^{Nt-1} r^*_A(x^*,y^*,t^* - p\times\Delta t) \quad (20)$$

for a given surface A in the case of 5-min spatial rainfall series located at $\{x^*,y^*\}$.

Thus, $Nt = 12$ for $D = 1$ h, ~~24 time-steps~~ $Nt = 24$ for $D = 2$ h and so forth. This procedure is illustrated in Fig. 3b. The 11 different time resolutions considered in this study range from 1 to 24 h (1, 2, 3, 4, 6, 8, 10, 12, 15, 18 and 24 h) and are all obtained from the original 5-min series.

3.2.3 Extraction of extreme rainfall: annual block maxima

The use of GEV distribution to model the extreme rainfall series requires using the block maxima procedure to extract rainfall extremes. It consists of defining annual blocks of observations separately for each of the 11 different time resolutions considered and to take the maxima within each block. A sample of 23 (1990–2012) annual maximum rainfall values $\{i(D, A)\}$ is thus obtained for each spatial aggregation and duration.

In summary:

- there are 13 reference locations;
- around each of the 13 reference locations, 12 areas of increasing size 1, 4, 9, 16, 25, 49, 100, 225, 400, 900, 1600 and 2500 km^2 are defined;
- for each of these 156 (13×12) areas, 11 time series of 23 (1990–2012) annual maximum values are constructed, corresponding to 11 different durations of rainfall accumulation 1, 2, 3, 4, 6, 8, 10, 12, 15, 18, 24 h.

4 Inferences of the individual components of the model

The proposed model has seven parameters: the temporal scale exponent (η), the three ARF parameters (a, b, ω) and the three GEV parameters (μ_{ref}, σ_{ref}, ξ_{ref}). After having tested different optimization procedures (most notably a global maximum likelihood estimation and the 2-step method proposed by Koutsoyiannis et al., 1998) a 3-step method was finally retained, since it gave the best results in the evaluation of the IDAF model (see Sect. 5). These three steps are explained in the following paragraphs (Sects. 4.1 to 4.3). For each step, an illustration based on the result obtained for the Niamey Aéroport station is given in Fig. 4.

4.1 Temporal simple scaling: estimation of η

The temporal scaling of the IDAF model is described by the η parameter. The inference of η is achieved in two steps. The first one consists in computing $k(q)$ for different moments q through a linear regression between the logarithm of the statistical moments of order q ($E[I^q]$) and the durations D (see Fig. 4a, left panel). Then, η is obtained by a linear regression between $k(q)$ and q (see Fig. 4a, right panel). At the Niamey Aéroport station, the value obtained for η is equal to -0.91.

4.2 GEV parameters: μ_{ref}, σ_{ref}, ξ_{ref}

The GEV parameters μ_{ref}, σ_{ref}, ξ_{ref} are estimated on the point samples, using the property that all normalized samples ~~$\{$~~$\{i(D,0)/D^{\eta}\}$~~$\}$~~ must come from the same distribution if simple scaling holds. All normalized samples are pooled in one single sample on which the GEV parameters are estimated (this methodology corresponds to the second step of the 2-step method proposed by Koutsoyiannis et al., 1998). Figure 4b illustrates this process at the Niamey Aéroport rain gauge: initial samples are displayed on the left panel, normalized samples are plotted on the right panel. The fitted GEV and the estimated GEV parameters are also given in this figure.

In comparison with fitting the GEV parameters ~~to one durationsamples only~~separately to each sample constituted for each duration, this method ~~takes advantage of (i) limiting sampling effect by increasing the sample size and (ii) using the information provided by all~~ aims at limiting sampling effects by fitting the GEV parameters on a single sample gathering all rainfall durations. The maximum Likelihood and the L-Moments methods were tested for estimating the GEV parameters. The estimation provided by these methods gave similar results, probably due to the large sample size. The results of the L-Moments method are presented here, this method being generally considered better than the MLE for the estimation of high quantiles when the length of the series are short (Hosking and Wallis, 1997).

4.3 Spatial scaling

The estimation of a, b, ω was carried out by minimizing the mean square difference between the empirical ARF (Eq. 10) and the model ARF (Eq. 12), as originally proposed by De Michele et al. (2001). Other scores (mean and max absolute error, bias, ...) and variables (difference between the observed and model mean areal rainfall) have been tried but gave poorer results in validation (Sect. 5). Figure 4c shows the comparison between the empirical ARF and the model ARF at the Niamey Aéroport station and the parameters obtained for the theoretical ARF model.

4.4 ~~Inference on regional samples~~Regional model

The point parameter inference (μ_{ref}, σ_{ref}, ξ_{ref} and η) has been performed on each of the 30 point rainfall series, which thus provide 30 IDF models. The complete IDAF model has been fitted to each of the 13 rain gauges CR. The obtained IDF and IDAF parameters do not display either any coherent spatial pattern or any trend over the domain, as may be seen in Figure 5. Sampling effects due to the small area and the short length of the series may explain this point, since a trend has been observed on a larger domain at the regional scale for daily rainfall (Panthou et al., 2012).

Assuming a spatial homogeneity of rainfall distribution (no spatial pattern), annual maxima series have been pooled together to obtain regional samples. The regional samples were used to fit the IDAF model over the domain in order to limit sampling effects. The point regional sample pools together the 30 rainfall samples directly provided by the 30 rain gauges $i(D,0)$; the 12 areal regional samples obtained for each of the 12 spatial resolutions $\{i(D,A); A = 1,\ldots,2500\,\text{km}^2\}$ result from pooling together the 13 individual series (CR rain-gauges) computed as explained in Sect. 3.

Table 1 presents the parameters obtained for the global IDAF model. The obtained GEV parameters are μ_{ref}= 40.6 mm h^{-1}, σ_{ref} = 10.8 mm h^{-1}, and ξ_{ref} = 0.1. When upscaled to the daily duration μ(24 h) = 2.29 mm h^{-1} (55.0 mm day^{-1}) and σ(24 h) = 0.61 mm h^{-1} (14.6 mm day^{-1}). It is worth noting that these latter values are coherent with those obtained for a much larger area in this region by Panthou et al. (2012, 2013) , working on the data of 126

daily rain gauges covering the period 1950-1990. Note also that the temporal scale exponent (η) is large (0.9), which means that the intensity strongly decreases as the duration increases. This is not surprising given the strong convective nature of rainfall in this region. Similar values of the temporal scaling exponents are obtained in regions where strong convective systems occur (Mohymont et al., 2004; Van-de Vyver and Demarée, 2010; Ceresetti et al., 2011) while lower values are obtained in regions where extreme rainfall is generated by different kinds of meteorological systems (for example in many mid-latitudes regions, see e.g. Menabde et al., 1999; Borga et al., 2005; Nhat et The dynamic scaling exponent is roughly equal to 1 which means that increasing the surface by a given factor leads to a similar ARF change than increasing the duration by the same factor (keeping in mind that this rule applies only to the range of time-space resolutions explored here).

5 IDAF model evaluation

The evaluation of the IDAF model is carried out in two successive stages. First each component used to build the final model (temporal simple scaling, ARF model and GEV distribution) is checked individually; then the global goodness of fit is tested using the Anderson–Darling (AD) and the Kolmogorov–Smirnov (KS) tests.

In Fig. 6 two series of graphs are plotted in order to verify whether the simple scaling hypothesis holds for the time dimension. On the left are the plots of ~~$\ln(E[i^q])$~~ $\ln(E[I^q])$ vs. $\ln(D)$ designed to check the log-log linearity between these two variables (Eq. 7); on the right are the plots of q vs. $k(q)$ aimed at checking the linearity between these two variables (Eq. 8). At all three spatial scales, there is a clear linearity of the plots, meaning that the two conditions for accepting the temporal simple-scaling hypothesis are fulfilled. Note that the graphs shown are those obtained on the regional samples for 3 different spatial scales only (point scale, 100 and 2500 km^2), but the quality of the fitting is similar for all the other spatial scales.

Simple scaling in space and dynamical scaling (e.g. the relationship between time and spatial scaling) are checked in Fig. 7. This figure compares the empirical ARFs (Eq. 10) computed on

the regional samples and the ARFs obtained with the model (Eq. 12) for all the space and time scales pooled together. With a determination coefficient (r^2) of 0.98, and a very small RMSE, it appears that the model restitutes very well the empirical ARF at all space and time scales, except at the hourly time step and for the three largest surfaces (900, 1600 and 2500 km^2), for which the model significantly underestimates the observed reduction factor. At such space–time scales the finite size of the convective systems generating the rain-fields creates a significant external intermittency (see Ali et al., 2003, on the distinction between internal and external intermittency). It thus seems that the simple scaling framework holds only as long as the influence of the external intermittency is negligible or weak. Consequently it is likely that the underestimation of the areal reduction factor by the simple scaling based model would be observed for larger space–time scales than the ones the AMMA-CATCH data set allows to explore.

Figure 8 illustrates that the global model is also able to reproduce very correctly the mean areal rainfall intensity over the whole time-space domain explored here, except again for the hourly time step and the largest surfaces.

As the IDAF model is primarily designed to estimate high quantiles, its ability to represent the mean is not a sufficient skill. It is thus of primary importance to evaluate its ability to also represent correctly high return ~~level~~ levels and extreme quantiles. This was realized by visually inspecting return level plots and by using Goodness Of Fit (GOF) statistical tests computed in a cross validation mode (all the stations are used to calibrate the model except one which is used to validate the model prediction). These tests are used to quantitatively assess how well the theoretical GEV distribution based on the IDAF model fits the empirical CDFs of the observed annual maxima for each spatio-temporal resolution. Each test provides a statistic and its corresponding p value. The p value is used as an acceptation/rejection criterion by fixing a threshold of non exceedance (here 1, 5, and 10 %).

The return level plots displayed in Fig. 9 for two reference locations and 3 time steps allow a visual inspection of the capacity of the global IDAF to fit the empirical samples. The p values of the two GOF tests are given in the inset caption. As could be expected, there is a significant dispersion of the results obtained on individual samples. The difficulty of reproducing correctly the empirical distribution when combining the smallest time steps with the largest areas is con-

firmed. While similar graphs were plotted for the other 11 reference locations, it is obviously difficult to obtain a relevant global evaluation from the visual examination of such plots.

Figure 10 aims at tackling this limitation by representing this information in a more synthetic way. In this figure the percentage of individual series for which the IDAF model is rejected by the Anderson–Darling GOF test is mapped for each duration and spatial aggregation for two levels of significance (1 and 10 %). Here it is worth remembering that we have 30 individual series for the point scale, and 13 different individual series for each of the 12 spatial scales, meaning that, for a given time step, the percentage of rejections/acceptations are computed from a total of 186 ($30 + 12 \times 13$) test values. Here again, the limits of the model for small time steps and large areas are clearly visible; one can also notice a larger number of rejections for small areas and the highest durations (duration higher than 12 h and area smaller than 25 km^2). Apart from that, the number of rejection of the null hypothesis remains low. The KS test (not shown) display similar result with a little less rejections of the null hypothesis. It thus appears fair to conclude that, over the range of space–time scales covered by the AMMA-CATCH network, a simple scaling approach allows for computing realistic areal reduction factors, the limit of validity being reached for areas roughly larger than 1000 km^2 at the hourly time step.

6 Discussion – conclusion

Up to now the rarity of rainfall measurements at high space–time resolution in Tropical Africa, had not permitted to carry out comprehensive studies on the scaling properties of rain-fields in that region. From 1990, the recording rain gauge network of the AMMA-CATCH observing system samples rainfall in a typical Sahelian region of West Africa at a time resolution of 5 min and a space resolution of 20 km, over an area slightly larger than $1^\circ \times 1^\circ$. This data set was used here for characterizing the space–time structure of extreme rainfall distribution, the first time such an attempt is made in this region where rainfall is notoriously highly variable.

Simple scaling was shown to hold for both the time and the space dimensions over a space–time domain ranging from 1 to 24 h and from the point scale to 2500 km^2; it was further shown that dynamical scaling relates the time scales to the space scales, leading to propose a global

IDAF model valid over this space–time domain, under the assumption that extreme rainfall values are GEV distributed.

Different optimization procedures were explored in order to infer the 7 parameters of this global IDAF model. A 3-step procedure was finally retained, the global IDAF model being fitted to a global sample built from all the different samples available for a given space–time scale. This model has been evaluated through different graphical methods and scores. These scores show that the areal reduction factors yielded by the IDAF model fit significantly well (in a statistical sense) the observed areal reduction factors over our space–time domain, except for the part of the domain combining the smallest time scales with the largest space scales. This limitation is likely related to the larger influence of the external intermittency of the rain-fields at such space–time scales.

Despite the growing accuracy of rainfall remote sensing devices, this study demonstrates that dense rain-gauge networks operating in a consistent way over long periods of time are still keys to the statistical modeling of extreme rainfall. In the numerous regions where rainfall is undersampled by operational networks and where satellite monitoring is not accurate enough to provide meaningful values of high rainfall at small space and time scales, dense networks covering a limited area may provide the information necessary for complementing the operational networks and satellite monitoring. In West Africa, south to the Niger site, AMMA-CATCH has been operating another site of similar size in a Soudanian climate since 1997 (Ouémé Catchment, Benin), providing ground for a similar study in a more humid tropical climate.

As mentioned in the discussion of Sect. 5, there is however a limitation of these two research networks, linked to their spatial coverage. Extending the area sampled by these networks to something in the order of $2^\circ \times 2^\circ$ would indeed allow studying more finely the effect of the limited size of the convective systems onto the statistical properties of the associated rain-fields. However, this means enlarging the area by a factor 4, making it much more costly and difficult from a logistical point of view to survey properly. For the years to come, AMMA-CATCH remains committed to operating both the Niger and the Benin sites for documenting possible evolutions of the rainfall regimes at fine space and time scales in the context of global change as well as for verifying whether the scaling relationships proposed here still hold for quantiles at

higher time periods. As a matter of fact, one strong hypothesis of the model proposed here is that the ARF is independent of the return period. This hypothesis seems verified for return periods smaller than the length of our time series, but it is not possible to infer whether this really holds for higher return periods. Therefore developing an IDAF model able to account for a possible evolution of the ARF with the return period level is a path that has to be explored, copulas being a candidate for such a development (e.g. Singh and Zhang, 2007; Ariff et al., 2012) .

It is also envisioned to test other IDAF model formulations based on alternative approaches for modeling the scale relationships, among which the method proposed by Overeem et al. (2010) seems of particular interest.

Appendix A:

A brief explanation of the transition between the simple-scaling framework used to described the space–time scaling of maximum annual rainfall (Eq. 13) and the GEV model used to model the statistical distribution of these maxima (Eqs. 15 to 17) is given here.

The random variables $I(D_{\text{ref}},0)$ and $I(D,A)$ are modeled by a GEV model:

$$\text{Prob}\{I(D_{\text{ref}},0) \le i(D_{\text{ref}},0)\} = \exp\left\{-\left[1+\xi(D_{\text{ref}},0)\left(\frac{i(D_{\text{ref}},0)-\mu(D_{\text{ref}},0)}{\sigma(D_{\text{ref}},0)}\right)\right]^{-\frac{1}{\xi(D_{\text{ref}},0)}}\right\} \quad \text{(A1)}$$

and

$$\text{Prob}\{(I(D,A) \le i(D,A)\} = \exp\left\{-\left[1+\xi(D,A)\left(\frac{i(D,A)-\mu(D,A)}{\sigma(D,A)}\right)\right]^{-\frac{1}{\xi(D,A)}}\right\}. \quad \text{(A2)}$$

Let introduce, $c = \lambda^{\eta} \times \text{ARF}(D,A)$ then Eq. (13) becomes:

$$I(D,A) \overset{d}{=} I(D_{\text{ref}},0) \times c \quad \text{(A3)}$$

and if Eq. (13) holds, then:

$$\begin{aligned}\text{Prob}\{I(D,A) \leq i(D,A)\} &= \text{Prob}\{I(D_{\text{ref}},0) \times c \leq i(D_{\text{ref}},0) \times c\} \\ &= \text{Prob}\{I(D_{\text{ref}},0) \leq i(D_{\text{ref}},0)\}\end{aligned} \tag{A4}$$

and

$$\text{Prob}\{I(D,A) \leq i(D,A)\} = \exp\left\{-\left[1+\xi(D_{\text{ref}},0)\left(\frac{i(D_{\text{ref}},0)-\mu(D_{\text{ref}},0)}{\sigma(D_{\text{ref}},0)}\right)\right]^{-\frac{1}{\xi(D_{\text{ref}},0)}}\right\}. \tag{A5}$$

By replacing $I(D_{\text{ref}},0)$ by $I(D,A)/c$ we obtain

$$\text{Prob}\{I(D,A) \leq i(D,A)\} = \exp\left\{-\left[1+\xi(D_{\text{ref}},0)\left(\frac{\frac{I(D,A)}{c}-\mu(D_{\text{ref}},0)}{\sigma(D_{\text{ref}},0)}\right)\right]^{-\frac{1}{\xi(D_{\text{ref}},0)}}\right\} \tag{A6}$$

or

$$\text{Prob}\{I(D,A) \leq i(D,A)\} = \exp\left\{-\left[1+\xi(D_{\text{ref}},0)\left(\frac{I(D,A)-\mu(D_{\text{ref}},0)\times c}{\sigma(D_{\text{ref}},0)\times c}\right)\right]^{-\frac{1}{\xi(D_{\text{ref}},0)}}\right\}. \tag{A7}$$

The equality between Eq. (A2) and Eq. (A7) gives:

$$\mu(D,A) = \mu_{\text{ref}} \times c \tag{A8}$$

$$\sigma(D,A) = \sigma_{\text{ref}} \times c \tag{A9}$$

$$\xi(D,A) = \xi_{\text{ref}}. \tag{A10}$$

Equations (A8) to (A10) correspond to Eqs. (15) to (17) in the main text.

Acknowledgements. This research was partly funded by the LABEX OSUG@2020 (ANR10 LABX56), partly by the French project ESCAPE (ANR10-CEPL-005), and partly by IRD and INSU through the support to the AMMA-CATCH observing system. Gérémy Panthou Ph.D. grant is funded by SOFRECO.

References

Ali, –A., Lebel, –T., and Amani, –A.: Invariance in the ~~spatial structure of sahelian rain fields at climatological scales, J. Hydrometeorol.~~Spatial Structure of Sahelian Rain Fields at Climatological Scales, Journal Of Hydrometeorology, 4, 996–1011, 2003.

Allen, R. and ~~Degaetano~~DeGaetano, A.: Areal Reduction Factors for Two eastern United States Regions with High Rain-Gauge Density, ~~J. Hydrol. Eng.~~Journal of Hydrologic Engineering, 10, 327–335, ~~2005~~ 2005.

Ariff, –N., Jemain, –A., Ibrahim, –K., and Wan Zin, –W.: ~~IDF~~ IDF relationships using bivariate copula for storm events in Peninsular Malaysia, ~~J. Hydrol., 470–471~~Journal of Hydrology, 470-471, 158–171, 2012.

Asquith, –W. H. and Famiglietti, –J. S.: Precipitation areal-reduction factor estimation using an annual-maxima centered approach, ~~J. Hydrol.~~Journal of Hydrology, 230, 55–69, 2000.

Awadallah, –A.: Developing ~~intensity–duration–frequency curves in scarce data region: an approach using regional analysis and satellite data, Engineering-London, 3~~Intensity-Duration-Frequency Curves in Scarce Data Region: An Approach using Regional Analysis and Satellite Data, Engineering, 03, 215–226, 2011.

~~Bara,~~

Bara, M., ~~Kohnov,~~ Kohnová, S., ~~Gal,~~ Gaál, L., Szolgay, –J., and ~~Hlavcov,~~ Hlavcová, K.: Estimation of IDF curves of extreme rainfall by simple scaling in Slovakia, ~~Contr. Geophys.~~ Contributions to Geophysics and Geodesy, 39, 187–206, 2009.

Bell, –F.: The ~~Areal Reduction Factor in Rainfall Frequency Estimation~~areal reduction factor in rainfall frequency estimation, Tech. –rep. 35, Institute of hydrology, Natural Environment Research Council, ~~UK~~UK, 1976.

Ben-Zvi, A.: Rainfall intensity-duration-frequency relationships derived from large partial duration series, Journal of Hydrology, 367, 104–114, 2009.

Bendjoudi, –H., Hubert, –P., Schertzer, –D., and Lovejoy, –S.: ~~Interpr~~Interprétation multifractale des courbes ~~intensit–dure-frquence des preipitations, CR~~ intensité-durée-fréquence des précipitations, C. R. Acad. Sci. ~~II A,~~ Paris, Sciences de la terre et des planétes / Earth & Planetary Sciences, 325, 323–326, 1997.

~~Ben-Zvi, A.: Rainfall intensity–duration–frequency relationships derived from large partial duration series, J. Hydrol., 367, 104–114, 2009.~~

Borga, M., Vezzani, C., and Fontana, G. D.: Regional rainfall depth–duration–frequency depth-duration-frequency equations for an Alpine region, Nat. Natural Hazards, 36, 221–235, 2005.

Burlando, P. and Rosso, R.: Scaling and muitiscaling models of depth–duration–frequency depth-duration-frequency curves for storm precipitation, J. Hydrol. Journal of Hydrology, 187, 45–64, 1996.

Castro, J. J., Crsteanu, Cârsteanu, A. A., and Flores, C. G.: Intensity–duration–area–frequency Intensity-duration-area-frequency functions for precipitation in a multifractal framework, Physica A A: Statistical Mechanics and its Applications, 338, 206–210, 2004.

Ceresetti, D.: Structure Spatio-Temporelle des Fortes Prspatio-temporelle des fortes précipitations: Application la Rgion Cà la région Cévennes Vivarais, Ph.D. thesis, Universitthesis, Université de Grenoble, Grenoble, 2011.

Ceresetti, D., Anquetin, S., Molinié, G., Leblois, E., and Creutin, J.: Multiscale Evaluation of Extreme Rainfall Event Predictions Using Severity Diagrams, Weather and Forecasting, 27, 174–188, 2011.

Coles, S.: An Introduction to Statistical Modeling of Extreme Valuesintroduction to statistical modeling of extreme values, Springer, London,;New York, 2001.

De Michele, C., Kottegoda, N. T., and Rosso, R.: The derivation of areal reduction factor of storm rainfall from its scaling properties, Water Resour. Res.Resources Research, 37, 3247–3252, 2001.

De Michele, C., Kottegoda, N., and Rosso, R.: IDAF (intensity-duration-area frequency) curves of extreme storm rainfall: a scaling approach, Water science and technology, 45, 83–90, 2002.

De Michele, C., Zenoni, E., Pecora, S., and Rosso, R.: Analytical derivation of rain intensity–duration–area–frequency intensity-duration-area-frequency relationships from event maxima, J. Hydrol. Journal of Hydrology, 399, 385–393, 2011.

Descroix, L., Genthon, P., Amogu, O., Rajot, J. L., Sighomnou, D., and Vauclin, M.: Change in Sahelian Rivers hydrograph: The case of recent red floods of the Niger River in the Niamey region, Global Planet. Change, 98–99and Planetary Change, 98-99, 18–30, 2012.

Di-Baldassarre, G., Montanari, A., Lins, H., Koutsoyiannis, D., Brandimarte, L., and Blschl, Blöschl, G.: Flood fatalities in Africa: from From diagnosis to mitigation, Geophys. Res. Lett. Geophysical Research Letters, 37, 1–5, 2010.

Gerold, L. and Watkins, D.: Short duration rainfall frequency analysis in Michigan using scale-invariance assumptions, J. Hydrol. Eng. Duration Rainfall Frequency Analysis in Michigan Using Scale-Invariance Assumptions, Journal of Hydrologic Engineering, 10, 450–457, 2005.

Gupta, –V. and Waymire, –E.: Multiscaling properties of spatial rainfall and river flow distributions, J. Geophys. Res.Journal Of Geophysical Research, 95, 1999–2009, 1990.

Hosking, —J. and Wallis, —J. R.: Regional Frequency Analysis: an Approach Based on L-Momentsfrequency analysis: an approach based on L-moments, Cambridge University Press, Cambridge ,UK, 1997.

Koutsoyiannis, –D., Kozonis, –D., and Manetas, –A.: A mathematical framework for studying rainfall intensity–duration–frequency relationships, J. Hydrol.intensity-duration-frequency relationships, Journal of Hydrology, 206, 118–135, 1998.

Lebel, -T., Sauvageot, -H., Hoepffner, -M., Desbois, -M., Guillot, -B., and Hubert, -P.: Rainfall estimation in the Sahel: the EPSAT-NIGER experiment, Hydrol. Sci.EPSAT-NIGER experiment, Hydrological Sciences, 37, 201–215, 1992.

Menabde, –

Menabde, M., Seed, –A.A., and Pegram, -G.: A simple scaling model for extreme rainfall, Water Resour. Res.Resources Research, 35, 335–339, 1999.

Mohymont, –

Mohymont, B., Demare, –Demarée, G. R., and Faka, -D. N.: Establishment of IDF-curves IDF-curves for precipitation in the tropical area of Central Africa – comparison Africa-comparison of techniques and results, Nat. Hazards Earth Syst. Sci.Natural Hazards and Earth System Science, 4, 375–387, ,2004.

Nhat, L., Tachikawa, Y., Sayama, T., and Takara, K.: A simple scaling charateristics of rainfall in time and space to derive intensity duration frequency relationships, Ann. J. Hydraul. Eng.Annual Journal of Hydraulic Engineering, 51, 73–78, 2007.

Overeem, —A., Buishand, —A., and Holleman, —I.: Rainfall depth–duration–frequency depth-duration-frequency curves and their uncertainties, J. Hydrol.Journal Of Hydrology, 348, 124–134, 2008.

Overeem, A., Buishand, T. A., and Holleman, I.: Extreme rainfall analysis and estimation of depth-duration-frequency curves using weather radar, Water Resources Research, 45, W10 424, 2009.

Overeem, A., Buishand, T. A., Holleman, I., and Uijlenhoet, R.: Extreme value modeling of areal rainfallfrom rainfall from weather radar, Water Resour. Res.Resources Research, 46, W09514, , W09 514, 2010.

Oyebande, -L.: Deriving rainfall intensity–duration–frequency intensity-duration-frequency relationships and estimates for regions with inadequate data, HydrologHydrol. Sci. J., 27, 353–367, 1982.

Oyegoke, S. and Oyebande, L.: A new technique for analysis of extreme rainfall for Nigeria, ~~Environ. Res. J.~~Environmental Research Journal, 2, 7–14, 2008.

Panthou, G., Vischel, T., Lebel, T., Blanchet, J., Quantin, G., and Ali, A.: Extreme rainfall in West Africa: ~~a~~ A regional modeling, Water ~~Resour. Res.~~Resources Research, 48, 1–19, 2012.

Panthou, G., Vischel, T., Lebel, T., Quantin, G., Pugin, A.-C., Blanchet, J., and Ali, A.: From pointwise testing to a regional vision: An integrated statistical approach to detect nonstationarity in extreme daily rainfall. Application to the Sahelian region, Journal of Geophysical Research: Atmospheres, 118, 8222–8237, 2013.

Papalexiou, S. and Koutsoyiannis, D.: Battle of extreme value distributions: ~~a~~ A global survey on extreme daily rainfall, Water ~~Resour. Res.~~Resources Research, 49, 187–201, 2013.

Ribstein, P. and Rodier, J.: La predetermination des crues sur des petits bassins saheliens inferieurs à 10 ~~km^2~~km2, Tech. rep., ~~ORSTOM~~ORSTOM, Laboratoire d'hydrologie, Montpellier, 1994.

Rodier, J. and Ribstein, P.: Estimation des caracteristiques de la crue decennale pour les petits basins versants du Sahel couvrant de 1 a 10 ~~km^2~~km2, Tech. rep., ~~ORSTOM~~ORSTOM, Laboratoire d'hydrologie, Montpellier, 1988.

Samimi, C., Fink, ~~A. H.~~A., and Paeth, H.: The 2007 flood in the Sahel: ~~causes~~Causes, characteristics and its presentation in the media and ~~FEWS NET~~FEWS NET, Natural Hazards and Earth System Sciences, ~~Nat. Hazards Earth Syst. Sci.,~~ 12, 313–325, ~~,~~2012.

Schertzer, D. and Lovejoy, S.: Physical ~~modeling and analysis of rain and clouds by anisotropic scaling multiplicative processes, J. Geophys. Res.~~Modeling and Analysis of Rain and Clouds by Anisotropic Scaling Multiplicative Processes, Journal of Geophysical Research, 92, 9693–9714, 1987.

Singh, V. and Zhang, L.: IDF Curves Using the Frank Archimedean Copula, Journal of Hydrologic Engineering, 12, 651–662, 2007.

Soro, G., Goula, ~~B.~~ B. T. A., Kouassi, F., and Srohourou, B.: Update of ~~intensity–duration–frequency~~ Intensity-Duration-Frequency curves for precipitation of short durations in tropical area of West Africa (cote d'Ivoire), ~~J. Appl. Sci.~~Journal Of Applied Sciences, 10, 704–715, 2010.

Tarhule, A.: Damaging ~~rainfall and flooding: the other Sahel hazards~~Rainfall and Flooding: The Other Sahel Hazards, Climatic Change, 72, 355–377, 2005.

Van-de Vyver, H. and Demarée, G. R.: Construction of Intensity-Duration-Frequency (IDF) curves for precipitation at Lubumbashi, Congo, under the hypothesis of inadequate data, Hydrological Sciences Journal-Journal des Sciences Hydrologiques, 55, 555–564, 2010.

Veneziano, D., Furcolo, P., and Iacobellis, V.: Imperfect scaling of time and ~~space–time rainfall, J. Hydrol.~~space-time rainfall, Journal of Hydrology, 322, 105–119, 2006.

Vischel, T., Quantin, G., Lebel, T., Viarre, J., Gosset, M., Cazenave, F., and Panthou, G.: Generation of ~~high-resolution rain fields~~ High-Resolution Rain Fields in West Africa: ~~evaluation of dynamic interpolation methods, J. Hydrometeorol.~~ Evaluation of Dynamic Interpolation Methods, Journal of Hydrometeorology, 12, 1465–1482, 2011.

Yu, P., Yang, T., and Lin, C.: Regional rainfall intensity formulas based on scaling property of rainfall, ~~J. Hydrol.~~ Journal of Hydrology, 295, 108–123, 2004.

Table 1. Obtained parameters for the global IDAF model (a) and corresponding GEV parameters values for the different durations D for the point scale A=0 (b)

μ_{ref}	σ_{ref}	xi	η	a	b	z	ω
40.60	10.81	0.10	-0.90	0.165	0.156	1.06	0.026

(a)

GEV Parameter	1h	2h	3h	4h	6h	8h	10h	12h	15h	18h	24h
μ (mm h^{-1})	40.60	21.68	15.02	11.58	8.02	6.19	5.05	4.29	3.50	2.97	2.29
σ (mm h^{-1})	10.81	5.77	4.00	3.08	2.14	1.65	1.35	1.14	0.93	0.79	0.61
ξ (-)	0.10										

(b)

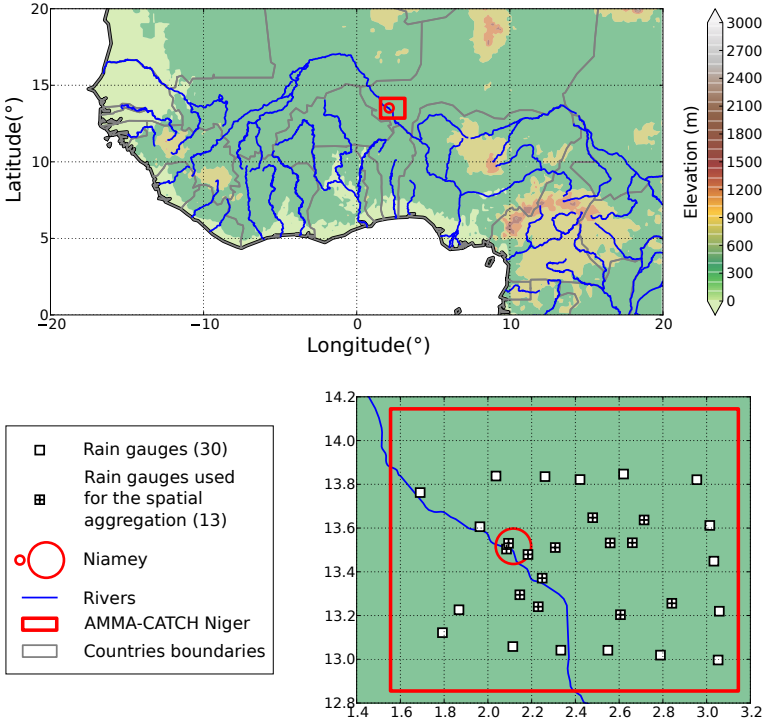

Figure 1. Study area. The background maps displays the elevation (meters).

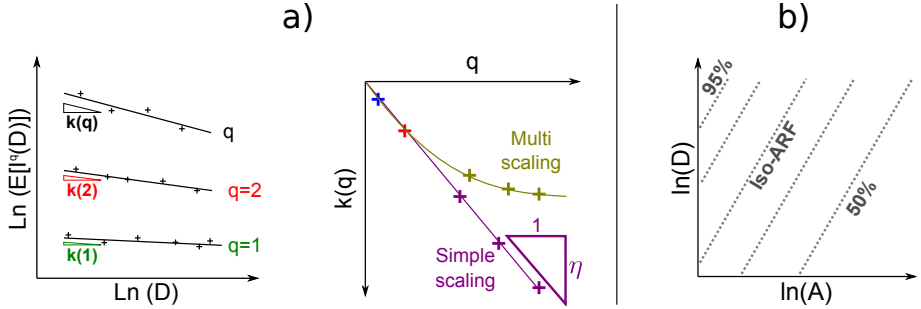

Figure 2. Visual model checks: **(a)** simple scaling; **(b)** ARF.

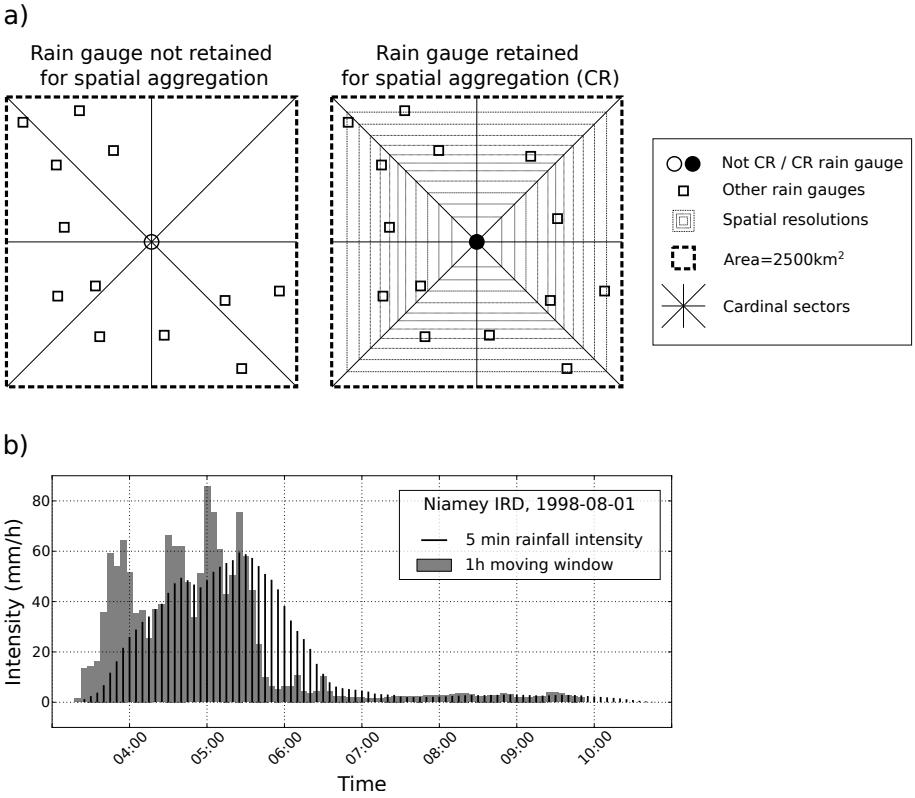

Figure 3. Examples of space and time aggregation used: **(a)** ~~time~~ spatial aggregation, **(b)** ~~spatial~~ time aggregation.

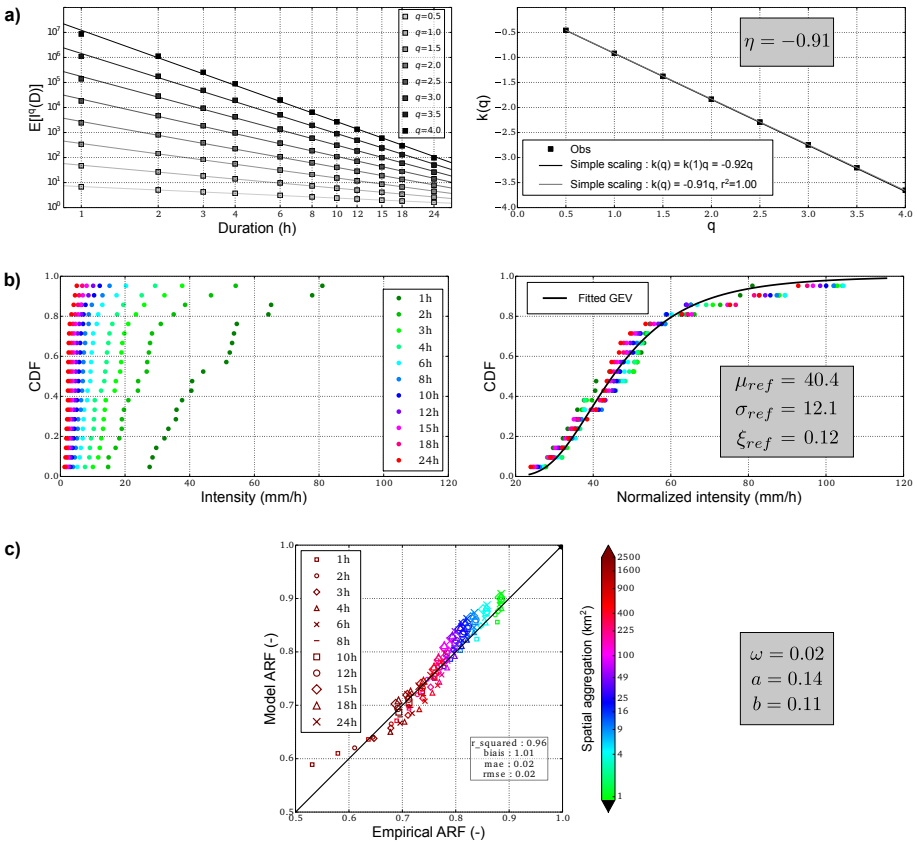

Figure 4. Example of IDAF model inference ~~: example~~ at the Niamey Aeroport rain gauge: **(a)** Checking of the temporal simple scaling conditions (left: linear relationship between the logarithm of the statistical moments of order q and the durations D, right: linear relationship between $k(q)$ and q) and estimation of the temporal simple scaling exponent; **(b)** left: empirical cumulative distribution of annual maxima, right: global fitting of the GEV parameters; **(c)** Comparison between empirical and modelled ARF.

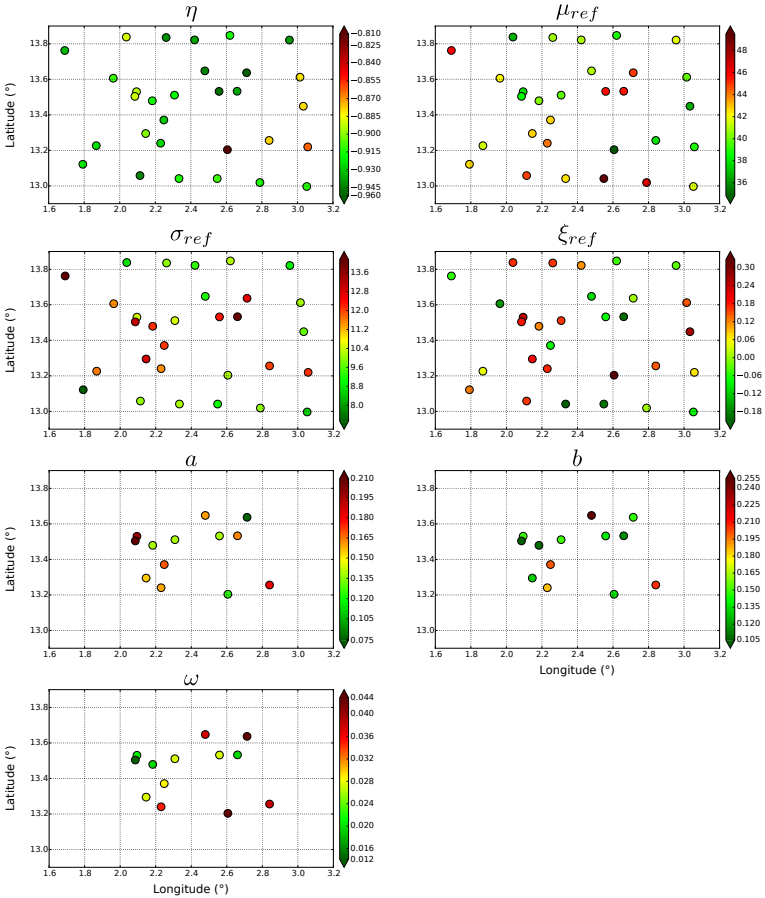

Figure 5. ~~Simple scaling checking:~~ Map of the obtained IDF parameters (η, μ_{ref}, σ_{ref} and ξ_{ref} fitted on the 30 rain gauges ~~series are pooled~~ samples) and IDAF parameters (~~global point sample~~η, μ_{ref}, σ_{ref}, ξ_{ref}, a, b and ω fitted on the 13 CR rain gauge samples).

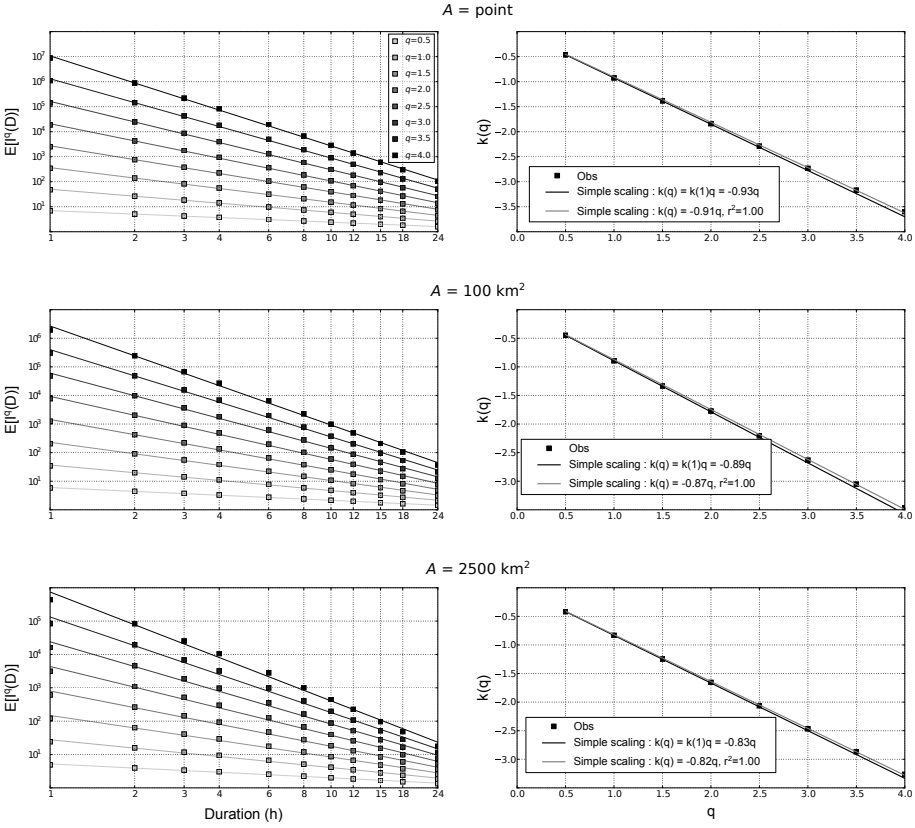

Figure 6. Checking of the temporal simple scaling conditions for the regional samples defined by the 30 available rain gauges for point resolution (top), and the 13 CR rain gauges (see Section 3.2.1) for the resolutions 100 km^2 (middle) and 2500 km^2 (bottom).

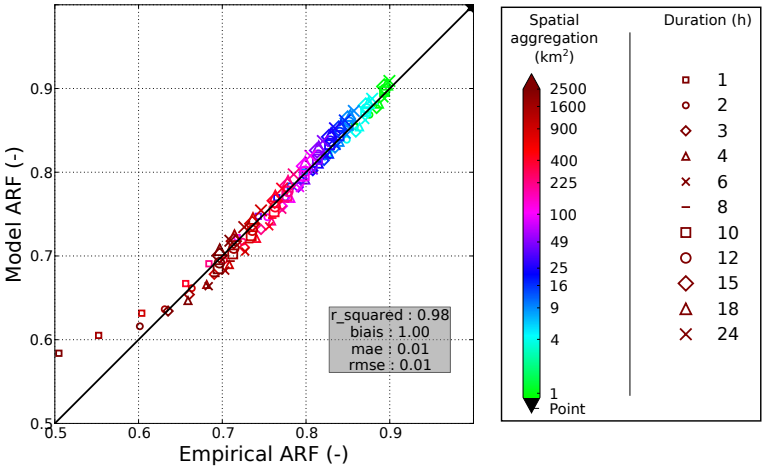

Figure 7. Comparison between empirical ARF (obtained with the ~~global sample~~regional samples: 30 rain gauges for point resolution and 13 CR rain gauges for other spatial resolutions) and ~~global~~ modelled ARF IDAF model.

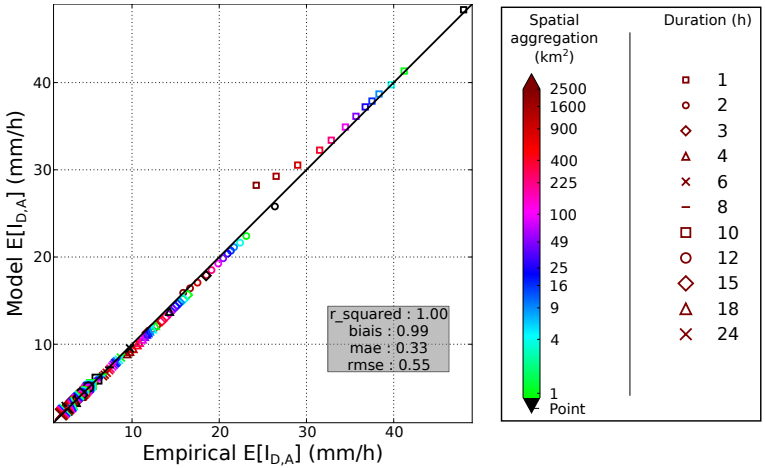

Figure 8. Comparison between empirical mean areal rainfall intensity (obtained with the ~~global sample~~regional samples: 30 rain gauges for point resolution and 13 CR rain gauges for other spatial resolutions) and global IDAF model for different spatio-temporal aggregations.

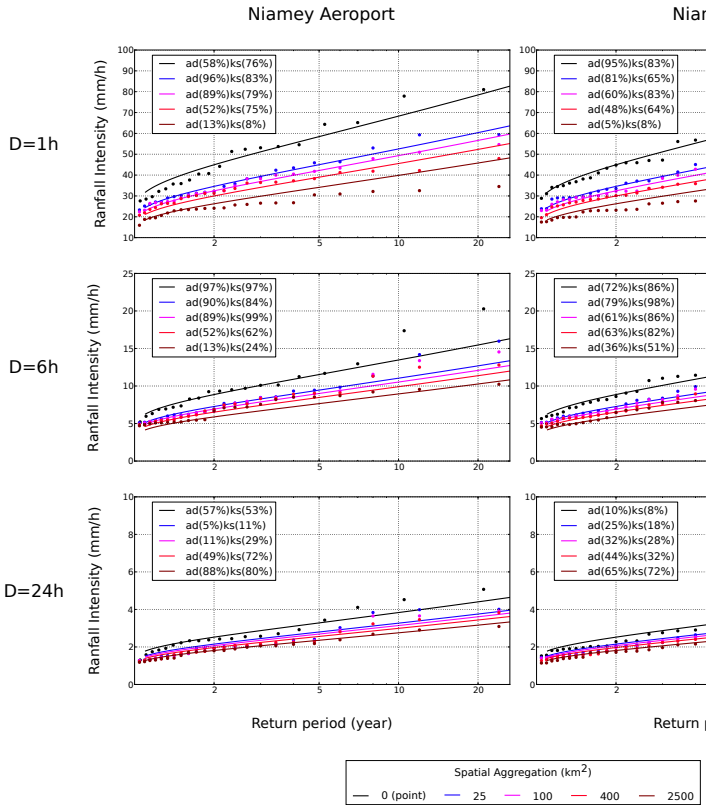

Figure 9. Empirical return level plot obtained at two rain gauges in comparison with the global IDAF model for different durations (1 h, 6 h and 24 h from top to bottom) and different spatial aggregations (from point to 2500 km^2).

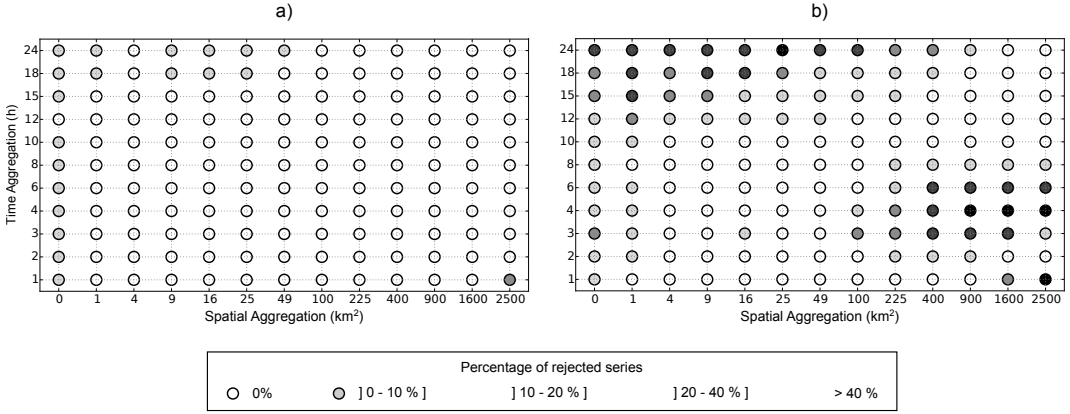

Figure 10. Anderson–Darling GOF test (cross validation): Percentage of rejected series for 1 % **(a)** and 10 % **(b)** significance level for the global IDAF model. Note that there are 30 series for the point scale ($0\,\mathrm{km}^2$) and 13 for the other spatial aggregation (rain gauges CR).